DOI:10.14753/SE.2022.2709

SEMMELWEIS EGYETEM

DOKTORI ISKOLA

Ph.D. értekezések

2709.

THANYAPORN SANG NGOEN

Fogorvostudományi kutatások
című program

Programvezető: Dr. Varga Gábor, egyetemi tanár, az MTA doktora
Témavezetők: Dr. Varga Gábor, egyetemi tanár, az MTA doktora
Dr. Földes Anna, tudományos munkatárs

DOI:10.14753/SE.2022.2709

A novel *in vitro* model for studying the molecular mechanisms of amelogenesis in physiological and pathological conditions

PhD thesis

Thanyaporn Sang-ngoen

Károly Rácz Doctoral School of Clinical Medicine

Semmelweis University

Supervisor: Gábor Varga, D.Sc.

Anna Földes, Ph.D.

Official reviewers: Balázs Sándor, D.M.D., Ph.D.

Hargita Hegyesi, Ph.D.

Head of the Complex Examination Committee: István Gera, D.M.D., Ph.D.

Members of the Complex Examination Committee: József Barabás, M.D., Ph.D.

Zoltán Rakonczay, D.Sc.

Budapest
2021

DOI:10.14753/SE.2022.2709

Table of Contents

DOI:10.14753/SE.2022.2709

DOI:10.14753/SE.2022.2709

Abbreviations

2D	two dimensional
3D	three dimensional
AE	anion exchanger
AI	amelogenesis imperfecta:
AMBN	gene coding for ameloblastin protein
AMELX	gene on X chromosome coding for amelogenin protein
AMELY	gene on Y chromosome coding for amelogenin protein
AMTN	gene coding for amelotin protein
AP	apical papilla
ASC	adult stem cell
BCECF-AM	2',7'-Bis-(2-Carboxyethyl)-5-(and-6)-Carboxyfluorescein, Acetoxymethyl Ester
BME	basement membrane extract
BMSC	bone marrow mesenchymal stem cell
CA	carbonic anhydrase
CF	cystic fibrosis
Cftr	gene coding for cystic fibrosis transmembrane conductance regulator
CFTR	cystic fibrosis transmembrane conductance regulator
Cldn	claudin
DF	dental follicle
DFSC	dental follicle stem cell
DIDS	4,4′-Diisothiocyano-2,2′-stilbenedisulfonic acid
DPSC	dental pulp stem cell
ECM	extracellular matrix
EGF	epidermal growth factor
ENAM	enamelin
ER	Endoplasmic reticulum
ERM	epithelial rests of Malassez
ESC	embryonic stem cell
FBS	fetal bovine serum

FGF	fibroblast growth factor
Hap	hydroxyapatite
H^+-ATPase	proton pump belongs to the P(3)-type ATPase family
H_2DIDS	dihydro-4,4'-diisothiocyanostilbene-2,2'disulfonic acid
hDFSC	human dental follicle stem cell
hDPSC	human dental pulp stem cell
HERS	Hertwig's epithelial root sheath
hPDLSC	human periodontal ligament stem cell
IEE	inner enamel epithelium
IGF	Insulin-like growth factor
KLK	kallikrein-related peptidase
MMP	matrix metalloproteinase
MMP-20	matrix metalloproteinase-20, enamelysin
mRNA	messenger Ribonucleic Acid
NBCe	electrogenic Na^+-HCO_3^- cotransporter
NHE	Na^+-H^+ exchanger
NKCC	Na^+-K^+-Cl^- cotransporter
NMDG	N-methyl-d-glucamine
OEE	outer enamel epithelium
ODAM	odontogenic ameloblast-associated protein
PCR	polymerase chain reaction
PDGF	platelet-derived growth factor
PDL	periodontal ligament
PDLSC	periodontal ligament stem cell
PiT	phosphate transporter
pHi	intracellular pH
SCAP	stem cells from apical papilla
SCPPPQ1	secretory calcium-binding phosphoprotein-proline-glutamine-rich 1 protein
SEM	standard error of the mean
SHED	stem cells from human exfoliated deciduous teeth.
SLC	solute carrier

DOI:10.14753/SE.2022.2709

Slc4a2	gene coding for anion exchanger 2 (AE2)
Slc4a4	gene coding for Na^+-HCO_3^- cotransporter (NBCe1)
Slc26a4	gene coding for pendrin Cl^--HCO_3^- exchanger
SR	stellate reticulum
TJP	tight junction protein
TGFβ	transforming growth factor beta

DOI:10.14753/SE.2022.2709

1. Introduction

Teeth play a vital role in mastication, proper vocalization for communication, and facial esthetics (1-3). They are complex organs, as shown in figure 1, comprising three mineralized tissues: enamel, dentin and cementum; and soft tissue: dental pulp (1, 2). The tooth crown, the visible part, is covered by dental enamel. Enamel is acellular, inert, and rigid, but it is also fragile. Enamel is supported by an underlying layer, dentin, which is an elastic and avascular tissue. Dental pulp is the tooth's core and is supplied by the neurovascular system. The tooth root is protected by a bone-like mineralized connective tissue, cementum (2).

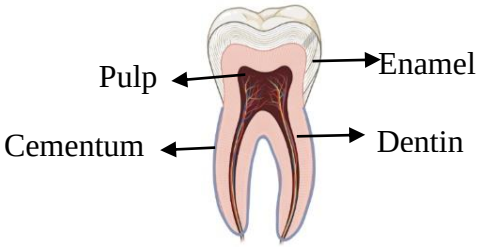

Figure 1. *The tooth is composed of enamel, dentin, pulp, supplied by nerves and blood vessels, and cementum. Adapted from "Tooth", by BioRender.com (2021). Retrieved from https://app.biorender.com/biorender-templates. (4)*

Teeth are located in the oral cavity, which connects to other parts of the body. Hence, damage to or loss of a tooth can cause or contribute to systemic diseases and affect overall health and well-being (1, 5). Treatments for tooth defects or loss are needed to improve human health. Currently, tooth defects and loss are restored by synthetic materials that cannot completely replicate the function of the natural tooth (5). Therefore, alternative treatments are required for tooth restoration, which better match the physiological state. Tooth repair and regeneration by tissue engineering techniques are candidate methods that might potentially be used to restore tooth defects or substitute the tooth loss (1, 5, 6). However, this approach requires a detailed understanding of tooth development. Although this can be elucidated using animal or traditional cell culture models, recent *in vivo* and *in vitro* models have several limitations and may raise ethical concerns or might not fully represent the physiological state of the human body (7, 8).

DOI:10.14753/SE.2022.2709

1.1 Tooth development

Odontogenesis is the process of tooth development. In humans, primary teeth begin to form during week six *in utero*, and permanent teeth start to develop during the twentieth week *in utero*. Tooth formation continues up to five years after birth (2, 9, 10). The process of tooth formation requires an orderly reciprocal interaction between the primitive oral epithelium and the ectomesenchyme or dental mesenchyme (2, 11-13). Signaling molecules that mediate this interaction include fibroblast growth factor (FGF), bone morphogenetic protein (BMP), hedgehog, and wingless protein families (11, 13, 14). The primitive oral epithelium originates from the oral ectoderm, while the ectomesenchyme arises from the neural crest (2, 11). Tooth formation begins at the thickening of the primary epithelial band, named dental placode, where the developing tooth will emerge (Figure 2A) (2, 13). From this step, the morphological features of these epithelial cells during tooth development can be distinguished and divided into three stages: the bud stage, the cap stage, and the bell stage (Figure 2) (2, 11, 12).

In the bud stage, a dental placode proliferates downwards to ectomesenchymal cells and forms a bud-liked structure called a tooth bud (Figure 2B). This tooth bud is attached to the oral epithelium by the dental lamina (13, 15). The ectomesenchymal cells then start to cluster around the tooth bud (2, 16). The tooth bud continues growing and exhibits a cap shape named the enamel organ (Figure 2C) (2, 11). The condensed ectomesenchymal cells beneath the cap, the dental papilla, will give rise to dentin and pulp, while the ectomesenchymal cells encapsulating the enamel organ, referred to as the dental follicle or sac, produce the tooth-supporting structures (15). The enamel organ, dental papilla, and dental follicle are together called the dental organ or tooth germ (2). The cap is composed of two different cell morphologies. The cuboidal cells covering the sides of the cap are called the outer enamel epithelium (OEE), and the low columnar-shaped cells lining the inner part of the cap are called the inner enamel epithelium (IEE) (2, 17). These two epithelial layers meet and form the cervical loop (17). The cap is filled with star-shaped (stellate) cells forming the stellate reticulum (SR) (2).

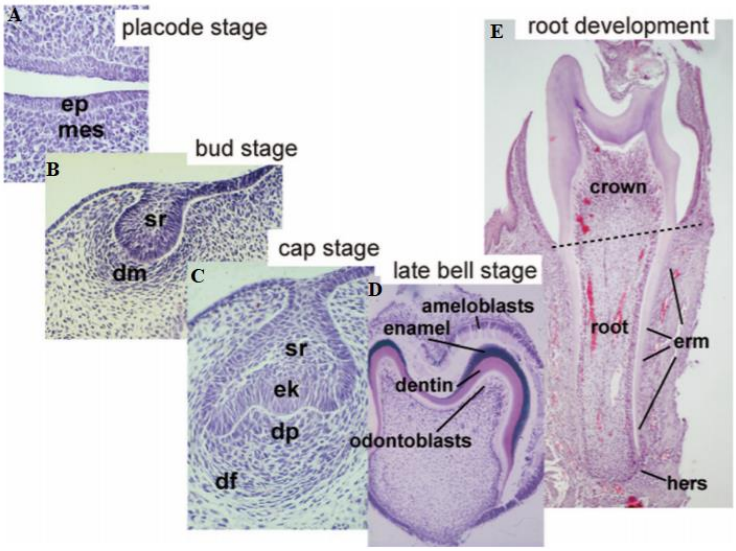

Figure 2. *The histology of tooth development. Tooth development begins when the dental epithelium thickens (A), followed by bud (B), cap (C), bell stage (D), and root development (E), respectively. ep: epithelium; mes: ectomesenchyme; sr: stellate reticulum; dm: dental mesenchyme; dp: dental papilla; df: dental follicle; ek: enamel knot; erm: epithelial cell rests of Malassez; and hers: Hertwig's epithelial root sheath. Adapted from (Thesleff & Tummers, 2009) (18).*

There is also a cluster of undifferentiated epithelial cells inside the enamel organ, known as the enamel knot. The enamel knot is thought to be a signaling center that regulates the formation of the tooth cusp (2, 11, 16). The number and location of the enamel knots indicates the number and location of the cusps (2, 19). At the late cap stage, the epithelial cells proliferate and deepen into ectomesenchyme, so the shape of the tooth germ changes from cap to bell (Figure 2D). The bell stage requires two changes in terms of morphodifferentiation, which determines the future shape of the tooth, and histodifferentiation, in which the cells transform into functional cells such as ameloblasts and odontoblasts (2, 11). During this stage, ameloblast cells form enamel, and odontoblast cells form dentin (15, 16). When the total size of the crown is accomplished, the dental lamina disintegrates and detaches the tooth germ from the oral epithelium (2, 11).

After crown formation, the cervical loop cells begin to proliferate downwards to form a double-layered epithelial structure named Hertwig’s epithelial root sheath (HERS) (Figure 2E) (2, 20). This root sheath is believed to guide the root formation and induce

the differentiation of odontoblasts. The limited growth of HERS determines the root length (19, 20). The disintegration of HERS results in the formation of the epithelial network called the epithelial rests of Malassez (ERM) (Figure 2E) (19). Once the tooth root formation is initiated, the dental follicle cells differentiate into cementoblasts, fibroblasts, and osteoblasts to form cementum on the root surface, periodontal ligament, and tooth-supporting bone respectively (2, 11, 19). In addition, the tooth begins to move vertically to erupt into the oral cavity (11).

1.2 Tooth enamel

Tooth or dental enamel is the translucent outer part of the tooth crown that is visible in the oral cavity. Its color varies from light yellow to greyish brown due to the variation of its thickness and the underlying yellow dentin, which reflects through it (2). Enamel is the hardest calcified tissue in the human body because of its high mineral composition and organized structure. It differs from other mineralized tissues such as bone in its origin, lack of vital cells, and absence of collagen (21). Enamel is mainly comprised of minerals (96% by weight), a small amount of water (3%), and organic material (1%) (2). The inorganic part of the enamel consists of carbonated hydroxyapatite (Hap) crystals containing large amounts of calcium ion (Ca^{2+}). These crystals are long, ribbon-like structures and grouped as rod or interrod enamel depending on the orientation of the crystals. The border between the rod and interrod enamel contains organic material referred to the rod sheath (2, 22). These features of the structural organization and chemical composition of enamel support its strength in withstanding the large mechanical forces during mastication (2, 21, 23). Although enamel has high strength, it is also brittle and cannot repair itself because the ameloblasts responsible for enamel secretion are lost upon tooth eruption (21).

1.2.1 Enamel formation

The enamel formation process, amelogenesis, begins at the bell stage of odontogenesis when the IEE cells differentiate into ameloblast cells (2). IEE cells are initially orchestrated by the underlying mesenchymal cells or dental papillae. Then, they gradually change from cuboidal to columnar shape (2). Ameloblasts play a primary role in mediating the process of enamel formation. They secrete enamel matrix proteins and maintain a favorable environment for mineralization (17, 24). The process of

amelogenesis has two distinct stages, the secretory and maturation stages, with a short transition stage between them (17, 25). During these stages, amelogenesis requires cellular proliferation and differentiation, precise sequential epithelial-mesenchymal interactions, secretion of the specific matrix proteins, ion transport, and the precipitation and alignment of enamel crystals (2, 21, 26). Consequently, the morphology of ameloblasts changes according to their specific functional roles in each stage (Figure 3)(2, 24).

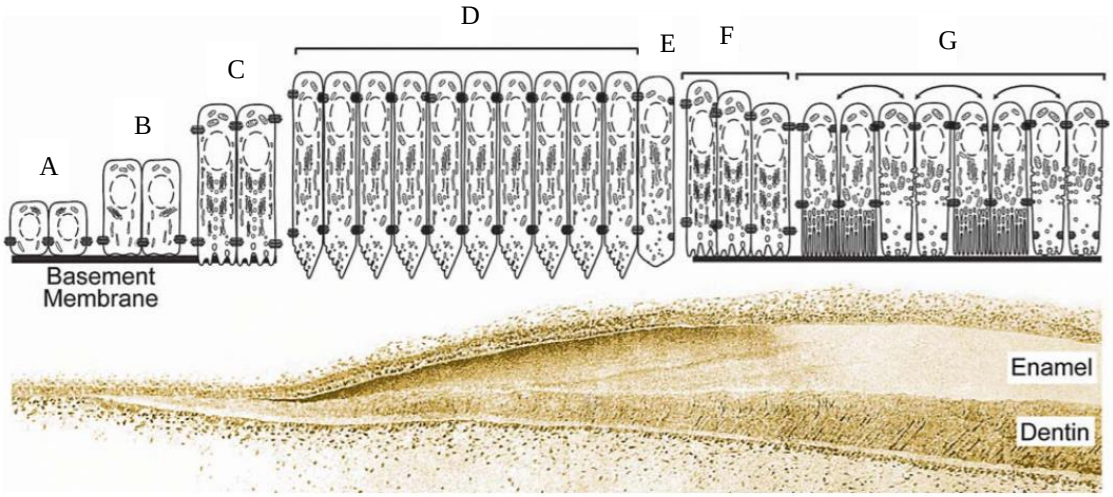

Figure 3. *Changes in ameloblast morphology during amelogenesis. Initially, the cells of the inner enamel epithelium (A) increase in height as differentiating ameloblasts (B). Presecretory ameloblasts initially form processes for secreting enamel proteins (C). Secretory ameloblasts develop Tomes' processes and secrete proteins at the mineralization front (D). At the end of the secretory stage, ameloblasts lose their Tomes' processes (E). During the transition stage, the ameloblasts diminish in height (F). Maturation ameloblasts modulate between ruffled and smooth-ended phases according to their function (G). Adapted from (Hu et al, 2007) (27).*

1.2.1.1 Secretory stage

IEE cells differentiate into secretory ameloblasts by elongating and shifting their nuclei to the basal pole of the cell (Figure 3A-D)(2). Their height (basal-apical distance) is commonly around 70 μm, but they can reach 90 μm (21). In addition, the protein synthesis apparatus, including the Golgi complex, rough endoplasmic reticulum, and mitochondria,

significantly increases (24). At the apical end of the ameloblast appears a triangular-shaped cytoplasm extension. This unique structure is called the Tomes' process and is significantly involved in the exocytosis of vesicles containing matrix proteins and the organization of the growing crystals (17, 28). In addition, secretory ameloblasts are tightly held together by junctional complexes and these form a selectively permeable barrier for ions transport between the environment and enamel matrix. Therefore, the secretory stage ameloblasts are functionally and morphologically polarized (2, 24).

The main function of secretory ameloblasts is to synthesize and secrete structural enamel matrix proteins, including amelogenin, ameloblastin, and enamelin. These proteins are essential for initiating calcification and controlling the growth of enamel crystals (29). Amelogenin is the most abundant enamel matrix protein; it accounts for approximately 80-90% of the total enamel protein (27, 30). It is crucial for controlling the normal growth and orientation of the enamel crystals (31, 32). Ameloblastin comprises approximately 5% of the total enamel protein (27, 33). Ameloblastin knock-out mice show a detachment of the ameloblasts from the enamel surface, suggesting that ameloblastin is a cell adhesion molecule maintaining the mineralization front (34). Enamelin is the least abundant protein, approximately 3-5% of total enamel protein (27, 35). This protein is only found at the mineralization front, suggesting that it is involved in elongating the enamel crystals or shaping minerals into enamel ribbons (27, 36, 37). The expression of amelogenin greatly decreases in the maturation stage, in which the entire thickness and volume of enamel is ultimately formed (38). The other two proteins, ameloblastin and enamelin, are believed to follow the same expression pattern as amelogenin (21). Mutations in the genes coding for amelogenin (AMELX, AMELY), ameloblastin (AMBN), and enamelin (ENAM) can cause amelogenesis imperfecta (AI). These gene defects impede the secretory stage of enamel formation, resulting in a thin enamel layer or even the absence of enamel, defined as a hypoplastic type of AI (34, 35, 39-42). Mutations in ENAM seem to be the most frequent known cause of AI (23, 35).

During the secretory stage, ameloblasts continuously secrete and deposit enamel proteins on the existing enamel surface, followed by a radial movement away from the place of secretion. This event increases the thickness of the enamel layer and relates to the elongation of enamel crystals (2).

Additionally, the proteolytic degradation of the structural proteins, particularly amelogenin, begins in this stage and is mediated by the enamel-specific proteolytic enzyme enamelysin (matrix metallopeptidase 20, MMP-20). The ameloblast expresses it during the secretory and early maturation stages; however, its expression is dominant in the secretory stage (43, 44). The *Mmp20* null mouse exhibits abnormal enamel, consisting of a thin layer with an altered enamel rod pattern, detached from the dentin layer (45). Evidently, protein degradation is an essential aspect of proper enamel formation (21, 25).

1.2.1.2 Transition stage

After the entire thickness of the immature enamel has been built, the morphology of the secretory ameloblasts changes. They become shorter, lose their Tomes' processes, and reduce the number of intracellular organelles (Figure 3F) (2). Additionally, the expression of enamel matrix proteins coding genes such as *AMELX*, *AMELY*, *AMBN*, and *ENAM* decreases. At the same time, the expression of genes involved in ion transport, proteolysis, and pH homeostasis increases (46-48).

1.2.1.3 Maturation stage

Maturation stage ameloblasts are shorter than secretory ameloblasts but still maintain their apical-basal polarity. Their apical surface cyclically changes between ruffle-ended and smooth-ended appearances (Figure 3G) (49). Ruffle-ended ameloblasts show a distinct apical striated or ruffled border related to mitochondria and endocytosis (24, 50). The junctional complexes tightly connect ruffle-ended ameloblasts at their apical ends, but the basal junctions are leaky. In contrast, smooth-ended ameloblasts show a complete absence of the distal ruffled border. They possess leaky apical junctions but tight basal junctions. Associated with the different morphologies of ruffle-ended and smooth-ended ameloblasts, they perform different functions (21, 49, 51). Ruffle-ended ameloblasts mediate mineral transport, including calcium and phosphate, into the enamel space and neutralize the protons released during hydroxyapatite (Hap) crystal formation. Smooth-ended ameloblasts allow the passage of water and protein fragments (21, 24, 49, 51).

Although maturation ameloblasts show reduced secretion of enamel matrix proteins, some proteins, such as amelotin, odontogenic ameloblast-associated protein (ODAM), and secretory calcium-binding phosphoprotein-proline-glutamine-rich 1 (SCPPPQ1) are still secreted (52-57). The expression of the amelotin gene (*AMTN*) was initially discovered in an analysis of mRNA expression from dental tissues in mice (53).

The possible role of amelotin has been suggested as a cell adhesion tightly binding ameloblasts to the mineral of enamel (52, 58). The AMTN-deficient mice produced weak, hypomineralized enamel and abnormal enamel structure (59). ODAM was previously called Apin because it was isolated from the amyloid of Pindborg odontogenic tumors. This protein might be involved in an adhesive mechanism and regulates enamel protease MMP-20 (55-57, 60). The individual role of SCPPPQ1 is not known; however it is suggested that, together with amelotin and ODAM, it mediates the attachment of ameloblast cells to the mineralized enamel (54). These three enamel proteins have been discovered only recently, and more detailed studies of their functions in amelogenesis are still needed.

The increase in the enamel thickness ceases at the end of the secretory stage. At this point, the enamel is hypomineralized and contains a large amount of enamel protein cleavage products. Hence, proteolytic degradation is required to harden the enamel layer in the subsequent maturation stage. Maturation ameloblasts secrete kallikrein-related peptidase 4 (KLK4), which mainly degrades enamel structural proteins. The residual protein fragments are resorbed and removed from the tissues by ameloblasts (2, 61-63). When the matrix proteins disappear, their byproducts are replaced by fluid, creating a highly hydrated and porous tissue. This tissue then becomes much less hydrated, less porous, and more rigid as a result of crystal growth. This process requires the degradation and removal of matrix proteins to allow the deposition of mineral ions (25, 63). Mature enamel primarily comprises 37% calcium (Ca^{2+}) and 17% phosphate (PO_4^{3-}) by weight. Other mineral components, e.g. sodium (Na^+), magnesium (Mg^{2+}), potassium (K^+), chloride (Cl^-), and fluoride (F^-), are also found but in tiny proportions (25, 62, 63). These elements are transported from the blood circulation across ameloblasts, forming an epithelial barrier, and are deposited in the enamel space. Other substances, including bicarbonate ions (HCO_3^-), are transported to neutralize the protons (H^+) released during crystal growth (21, 64-67).

1.2.2 pH regulation during amelogenesis

During the maturation stage, the deposition of calcium and phosphate ions occurs in an enamel-forming space that is mildly acidic (50, 64, 68). However, some studies have found an extracellular pH level ranging from acidic to slightly above neutral during enamel formation (68-70). It is believed that the acidic environment is caused by H^+ ions

released from hydroxyapatite crystal formation (24, 50, 62, 64, 65, 68, 71). During the secretory stage, amelogenin serves a crucial role in pH buffering. However, amelogenin is only present during the secretory phase. Thus, other buffer systems must modulate the pH of the enamel space during the maturation stage.

Based on recent studies, maturation-stage ameloblasts provide the key buffering system by secreting HCO_3^- ions to maintain the neutral pH of the enamel-forming area (24, 62, 64, 71). Ameloblasts produce HCO_3^- in the cells by carbonic anhydrase (CA) or transport from the blood circulation by active transport through specific transporters, namely the anion exchanger (AE2), Na^+-HCO_3^- cotransporter (NBCe1), Na^+-H^+ exchanger (NHE1), pendrin (Slc26a4), and cystic fibrosis transmembrane conductance regulator (CFTR) as shown in Figure 4 (72-75).

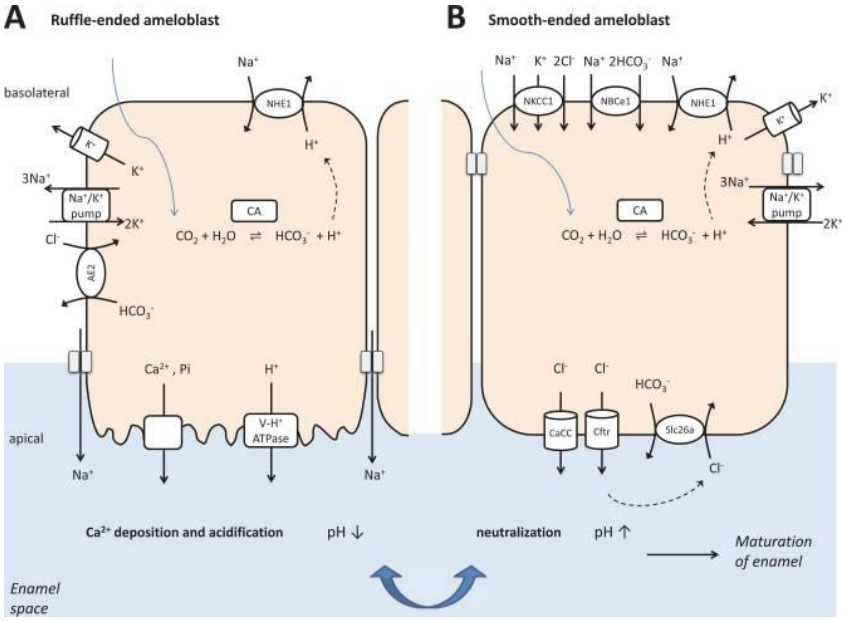

Figure 4. *A model illustrating pH modulation during amelogenesis by intracellular carbonic anhydrase and ion transporters located on the apical and basolateral membranes of ruffle-ended (A) and smooth-ended (B) ameloblasts. Adapted from (Racz et al., 2018) (76).*

CAs are zinc-containing metalloenzymes that catalyze the reversible reaction of carbon dioxide and water to form carbonic acid, which quickly splits into H^+ and HCO_3^- (77, 78). There is evidence that Cas are involved in pH regulation during enamel

formation (72-75, 79). Among the CA gene family, CA2 and CA6 are significantly upregulated in maturation ameloblasts compared to secretory ameloblasts (46, 48). CA2 generally localizes around the apical border of rough-ended ameloblasts (21, 71, 73). Due to its specific localization, the role of CA2 may be coupled with proton pumps, e.g., V-type ATPase (64, 68, 80). The expression of CA6 in ameloblasts has also been reported; however, its exact localization and function are still unclear (38, 46, 48, 74).

Electrolyte transporters in the SLC4 gene family play a significant role in pH regulation by transporting bicarbonate (17, 21). Anion exchangers or solute carrier 4 proteins (SLC4s) are responsible for exchanging one monovalent anion with another across the membrane, normally Cl^- and HCO_3^-(81). Among three identified in ameloblasts (AE1, AE2, and AE3), AE2, encoded by *Slc4a2* is mostly found in maturation ameloblasts (46, 48, 66, 67, 80, 81) and is located at the basolateral membrane (80, 82, 83). It transports intracellular bicarbonate out of the cell in exchange for extracellular $Cl^–$ and thus provides a source of intracellular Cl^- (65, 81). Mutations in the *Slc4a2* gene in mice cause the teeth to have a less mineralized enamel, an abnormal enamel structure, and show rapid wear (82).

Another member of the SLC4 gene family, the *Slc4a4* gene in mice, codes for NBCe1. NBCe1 is an electrogenic sodium bicarbonate cotransporter (21, 84). It transports Na^+ and HCO_3^- together across the membrane. The expression of NBCe1 is localized on the basolateral membrane in both secretory and maturation ameloblasts; nevertheless, its expression is highest during maturation stage (21, 46, 71, 83, 85). NBCe1$^{–/–}$ mice produced severely hypomineralized, weakened enamel with an atypical prismatic architecture (85). Evidently, NBCe1 is necessary for normal enamel development (83, 85).

The other product of CA activity, H^+, can be removed via an Na^+/H^+ exchanger such as NHE1 (21). NHE1, encoded by the *Slc9a1* gene, prevents intracellular acidification by exporting H^+ in exchange for Na^+ (66, 80). The expression of NHE1 is found on the basolateral membrane (66, 80). Another way to remove H^+ from the cell is via a V-type H^+-ATPase pump (21). H^+-ATPases are localized on the apical border of maturation-ameloblasts (80) which is surprising as this location would cause acidification of the enamel space, the opposite of what is required.

The expression of solute carrier 26A family members Slc26a3/Dra, Slc26a6/Pat-1, and Slc26a4/pendrin has been reported in rodent ameloblasts (86, 87). The proteins encoded by these genes are anion exchangers involved in the exchange of Cl^- and HCO_3^- (86-88). Their expression is found at the apical membrane of maturation ameloblasts (86, 87).

CFTR is a cAMP-regulated chloride channel (89, 90). It can be found at the apical membranes of epithelia in many organs, e.g. pancreatic ducts, salivary gland, uterine, etc. (90-93). CFTR is involved in HCO_3^- secretion (89-93). The expression of CFTR is maintained during amelogenesis and there is a significant upregulation at the maturation stage (46, 48). CFTR has been found on the apical membrane of maturation ameloblasts in the rodent enamel organ (89). The main function of CFTR has been suggested to be the export of intracellular Cl^- to the enamel matrix, and then Cl^- returns to the cell in exchange for HCO_3^- via anion exchangers such as the transporters encoded by *Slc26a* gene family (64, 84). Mutations in the *Cftr* gene in animal studies lead to abnormal enamel formation, including hypomineralization, abnormal crystal growth, and premature enamel degeneration (94-98). In humans, a mutation of the *CFTR* gene causes cystic fibrosis disease (CF) (99) and it has been observed that some CF patients have enamel abnormalities (100-103).

Recent evidence supports the function of ameloblasts in modulating extracellular pH during enamel formation. pH regulation is associated with electrolyte transporters located on the cell membranes of ameloblasts. Mutations in the genes coding for necessary transporters, as mentioned, lead to abnormal enamel structures and properties. Hence, the large number of H^+ ions liberated during Hap formation must be neutralized to sustain crystal growth and form normal enamel.

1.2.3 Dental fluorosis

Dental fluorosis is a developmental defect of dental enamel resulting from chronic and excessive fluoride exposure during enamel formation (9, 71, 104). This defect appears in deciduous dentition when fluoride exposure occurs during the embryonic period. In comparison, the fault appears in permanent dentition when the fluoride exposure occurs in 2-8 year old children (71). Fluoride is primarily recommended for preventing and managing dental caries because of its cariostatic capacity: it inhibits demineralization and stimulates remineralization around infected enamel areas (9, 104). The application of

either systemic or topical fluoride-containing products significantly decreases dental caries prevalence. On the other hand, increased prevalence of dental fluorosis has also been identified (9, 104).

Fluoride can affect any phase of amelogenesis. In the secretory stage, ameloblasts exposed to chronic high levels of fluoride change their morphology and the resulting enamel is decreased in thickness (104, 105). In addition, the production and function of proteolytic proteins are reduced (105, 106). Maturation-stage ameloblasts seem to be the most sensitive to fluoride. Several hypotheses for the diverse effects of fluoride have been proposed, such as the fluoride decreasing the matrix proteinase activity and the delayed modulation of pH by ameloblasts (104, 105). Excessive fluoride exposure may impair pH regulation during amelogenesis. Studies have demonstrated that fluoride expedites crystal formation; hence, many more H^+ ions are released, leading to a more acidic environment. The low extracellular pH upregulates the expression of ion transporters in the ameloblasts, and a large number of HCO_3^- ions are released to neutralize H^+. However, when the amount of H^+ exceeds the local buffering capacity, fluoride is convered to hydrogen fluoride and easily diffuses into the cytoplasm of the ameloblast cell following the concentration gradient caused by H^+(71, 107). Fluoride retention in the cytoplasm could induce ER stress, leading to decreased protein production, including the KLK4 proteinase, resulting in hypomineralized enamel (71). Furthermore, fluoride probably destroys the ameloblast cells by inducing oxidative stress, an intracellular imbalance between the production and accumulation of reactive oxygen species (ROS), and the elimination of these reactive products. Fluoride can inhibit the activity of antioxidant enzymes such as superoxide dismutase (SOD), glutathione peroxidase (GSH-Px or GPx), and catalase (CAT), bringing forth an overwhelming level of ROS production in the cells. Excessive ROS production gives rise to free radicals, which cause damage to intracellular organelles, including cell membranes, and activate the processes of cell death, such as apoptosis (108-113).

The clinical manifestation of dental fluorosis ranges from thin white horizontal lines across the teeth to a chalky white layer covering the entire enamel surface. In moderate to severe cases, the enamel surface shows pitting or yellow to light brown staining in the area of enamel erosion (9, 104). The various clinical manifestations of dental fluorosis are shown in Figure 5. The gold-standard diagnostic tool for evaluating

dental fluorosis in the clinic is the Dean index (104, 114). The index classifies the severity of the defect on the enamel surface with a score ranging from 0 to 10. The score is divided into four levels of severity: 0, 1-3, 4-5, 6-9 representing normal tooth, mild, moderate, and severe fluorosis respectively. The severity of the lesion depends on fluoride dose, duration of exposure, and the period of amelogenesis (26, 104, 105). The method for treatment of dental fluorosis is selected according to the severity of the lesion. For mild to moderate cases, tooth bleaching, microabrasion, or composite restoration is recommended. Prosthetic restoration such as crowns and veneers is suggested for severe cases (104, 115).

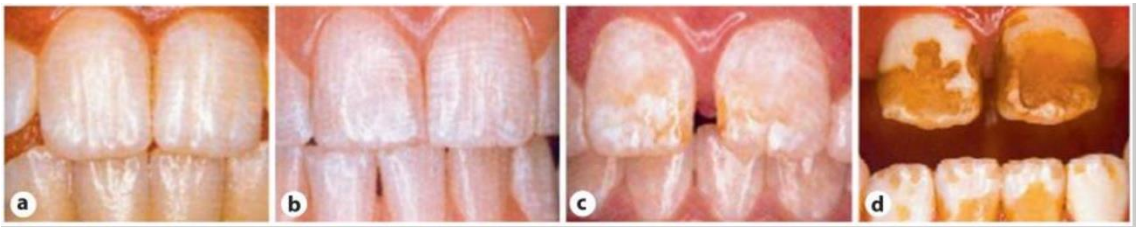

Figure 5. *The various clinical manifestations of fluorosis are categorized as mild (A), moderate (B, C), and severe (D). Adapted from (DenBesten & Li, 2011) (104).*

1.3 Stem Cells

A stem cell is a cell possessing clonal, self-renewing, and differentiation capacity (116, 117). Stem cells can be divided into three categories according to their differentiation potential: pluripotent, multipotent, and unipotent. Pluripotent stem cells can differentiate into any existent cell type. Multipotent stem cells can differentiate into cells from a single specific lineage, so they are lineage-specific. Lastly, unipotent stem cells can differentiate into one cell type, for example, spermatogonial stem cells (118). Alternatively, stem cells can be divided into two main groups: embryonic stem cells (ESCs) and adult stem cells (ASCs) (119, 120).

ESCs can be isolated from the inner cell mass of preimplantation embryos. They are pluripotent cells so that they can differentiate into almost all cell types and lineages under the proper signaling stimulation and environment (116, 117). Although ESCs have the capacity for differentiation, their use in regenerative therapy is limited due to ethical concerns and teratomas formed after transplantation (116, 121).

ASCs can be isolated from several tissues such as bone marrow, adipose tissue, skin, dental tissues, etc. (116). Bone marrow mesenchymal stem cells (BMSCs) can differentiate into a variety of cell lineages, e.g., adipocytes, osteocytes, chondrocytes, myocytes, hepatocytes, astrocytes, and neurons. Therefore, BMSCs are candidate stem cells for tissue regeneration and engineering (122-124). However, the limitations of using BMSCs include low differentiation potential, and the collection of these cells can cause pain (125, 126).

1.3.1 Dental tissue-derived stem cells

The oral cavity is a rich source of various stem cell types (Figure 6) that are easily accessed by noninvasive procedures (5, 127, 128). The first dental stem cells were successfully isolated from dental pulp (129). Dental pulp stem cells (DPSCs) have a high proliferation rate and play a role in pulp regeneration when they are stimulated. Furthermore, they can differentiate into other dental tissues such as dentin, cementum, periodontal ligament, bone, and non-dental tissues such as neurons and hepatocytes (5, 129, 130). Although many researchers have been investigating these cells, their use is still limited to *in vitro* and *in vivo* experimental studies.

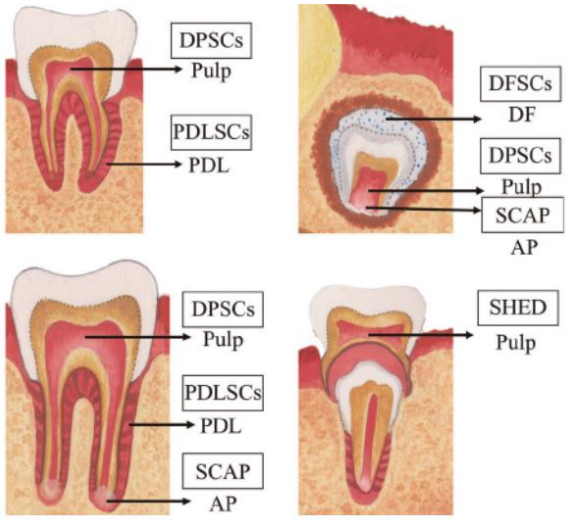

Figure 6. *The various types of stem cell derived from dental tissues, and their sources. AP: apical papilla; DF: dental follicle; DFSCs: dental follicle stem cells; DPSCs: dental pulp stem cells; PDL: periodontal ligament; PDLSCs: periodontal ligament stem cells; SCAP: stem cells from apical papilla; and SHED: stem cells from human exfoliated deciduous teeth. Adapted from (Khaseb et al., 2021) (131).*

More recently, stem cells from human exfoliated deciduous teeth (SHEDs) have been isolated from the pulp of baby teeth (132). SHEDs show a similar potential to DPSCs, but their proliferation rate is higher (119). Other DSCs, including periodontal ligament stem cells (PDLSCs) (133), dental follicle precursor cells (DFPCs) (134), and stem cells from apical papilla (SCAP) (135) have also been identified and characterized. In general, dental stem cells have a multi-differentiation potential. They are capable of differentiation into three cell lineages: osteo/odontogenic, adipogenic, and neurogenic. Nevertheless, they all tend to be capable of odontogenic development (127, 136-139). Dental stem cells are therefore a promising alternative for repairing and regenerating a range of dental tissues (140).

1.4 Cell culture techniques

Cell culture is a laboratory method for growing cells in near physiological conditions. The cell culture method provides a study model for cell biology, diseases, cellular toxicity of substances, drug discovery etc. (141, 142). Cultured cells can be divided into three different types: primary cells, transformed cells, and self-renewing cells. Primary cells are directly isolated from human or animal tissue by enzymatic or mechanical approaches. Transformed cells, referred to as cell lines, are immortalized cells generated naturally or by genetic modifications. They proliferate rapidly and largely maintain their characteristics. These cells are easy to handle and set up. Meanwhile, their normal functionality decreases with time in culture. These cells might not serve as an accurate model or replace human tissues, but they are optimal for initial proof-of-concept work development (116, 142, 143). Self-renewing cells or stem cells can differentiate into various types of cells and enable long-term maintenance *in vitro*. These cells usually maintain their physiological properties similar to what is observed *in vivo*.

All types of cell require suitable conditions for their growth. The major factors required for proper cell growth are the cell culture medium and its supplements, temperature, humidity, and gas concentration, including oxygen (O_2) and carbon dioxide (CO_2). Each cell type requires a specific culture medium. The culture medium typically contains amino acids, vitamins, glucose, and inorganic salts. Additionally, serum providing growth factors and hormones is added. For this purpose, fetal bovine serum

(FBS) is widely used. The environmental factors are achieved in incubators that provide the desired temperature, and CO_2 and O_2 levels. Cultures are usually maintained in a humidified atmosphere at 36-37°C containing 5-7% CO_2 (141, 142, 144).

1.4.1 Two dimensional (2D) cell culture

Cells grown on flat surfaces in conventional cell culture flasks, multi-well plates and Petri dishes can be described as two-dimensional (2D) static cell cultures. Single or mixed cell types, either primary cells or immortalized cell lines, are grown on flat plastic or glass substrates (Figure 7A), or on permeable plastic membranes (Figure 7B), and fed with specific culture media. The culture media are changed frequently to remove the metabolic waste and restore the nutrients. This technique is easy, convenient and low-cost (7, 143, 145). Thus, it has been widely used for investigating cell biology and physiological function, and for applications such as drug discovery and toxicity screening (145). *In vivo*, however, cells are surrounded by other cells and by extracellular matrix (ECM) in three-dimensional (3D) structures and nourished by nutrients in the blood circulation (146). Increasing amounts of evidence suggest that some aspects of the morphology and function of the cells that are seen *in vivo* are lost during 2D cell culture (7, 147, 148). These losses might yield unreliable data as compared with the cellular responses observed in intact organisms, and this could lead to invalid drug efficacy and toxicity tests (7, 146). Therefore, a more complex and more realistic 3D culture technique could help to resolve the inconsistencies between results obtained in 2D culture and in animal models or clinical trials (145).

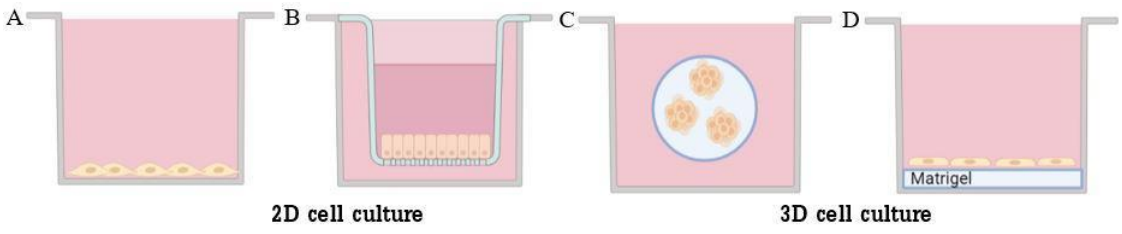

Figure 7. *Schematic diagrams of conventional (2D) cell culture (A), 2D cell culture on permeable Transwell filters (B), and 3D cell culture using Matrigel extracellular matrix: cells/spheroids can be cultured within the matrix (C), or on the surface of the matrix (D). Adapted from "Cell culture", by BioRender.com (2021). Retrieved from https://app.biorender.com/biorender-templates. (4)*

1.4.2 Three dimensional (3D) cell culture

Cells residing in living tissues interact with neighboring cells and the ECM to maintain their differentiation and the homeostasis of the tissues, but these interactions are lost during 2D culture (148). Therefore, various 3D culture techniques, such as multicellular spheroids, hydrogels, bioreactors, scaffolds, 3D bioprinting, etc., have been developed to better replicate the *in vivo* condition (147). The principal concept of the 3D culture technique is to allow the cells to form multilayer or spheroidal structures (7, 143). This re-establishes cell-cell and cell-ECM interactions resulting in a more physiologically relevant state that his more comparable to the *in vivo* environment (7, 143). 3D culture systems are widely used in cancer cell research, but 3D systems can also be used with stem cells, primary cells and cell lines (147). 3D cell cultures can provide a powerful model for insight into cell behavior, physiological mechanisms and differentiation, and may be applied to regenerative medicine and drug selection (146, 147). However, 3D cultures still require standard protocols to be determined for each cell type, and quantitative analysis methods, including imaging techniques (148).

1.4.2.1 Basement membrane extracellular matrix

Basement membrane matrix extracts, variously called Matrigel, Cultrex, or EHS matrix, form biological scaffolds (147, 149). They consist of soluble basement membrane proteins extracted from the Engelbreth-Holm-Swarm (EHS) tumor. The EHS tumor is a vast natural source of basement membrane components (149). The main constituents are laminin, type IV collagen, heparin sulfate proteoglycan and nidogen/entactin. Other components include proteases such as MMP-2 and MMP-9. The extract also contains growth factors, such as transforming growth factor beta (TGFβ), fibroblast growth factor (FGF), epidermal growth factor (EGF), platelet-derived growth factor (PDGF) and insulin-like growth factors (IGF) (149). Other proteins, including amylase transferrin and clusterin, can be found in the extract (149). All of these matrix substances promote cell attachment and reorganization into 3D structures (147). The matrix is stored as a frozen solution and thawed at 4°C overnight before use. The matrix becomes a gel at 24-37°C.

There are two techniques for matrix application. In the first, the matrix is plated on a flat surface. When the matrix becomes a gel, the cells are seeded onto the surface of

the gel (Figure 7D). In the second, the cells are mixed with the matrix before gelling (Figure 7C) (8, 150). When the cells contact the matrix, many cell lines or primary cells do not proliferate but differentiate. The differentiation of cells exposed to the matrix varies between different cell types. For example, the human submandibular gland (HSG) cell line forms acinar-like structures and secrete amylase when they are grown on a matrix (151, 152). Primary endothelial cells form capillary-like structures with lumen formation (153). The cells' differentiation is supported by their morphology and gene expression profiles. The matrix can be used with various cell types, including stem cells and cancer cells, and applied in model studies, tissue/organ transplantation, tissue repairs etc. (149).

1.5 Previous 2D functional ameloblast models

Most of our knowledge of mineral ion transport during amelogenesis is based on immunohistochemistry, chemical composition analysis, gene expression and the altered phenotypes of knock-out animals (24, 48, 65, 73, 79, 80, 82, 83, 85-87, 89, 94, 96, 97). In 2016, Bori and coworkers introduced a functional 2D ameloblast model showing the directional transport of HCO_3^- across the epithelium and the enhancement of HCO_3^- secretion in response to stimulants (66). The model was developed by seeding HAT-7 cells on permeable Transwell filters. HAT-7 is a cell line isolated from the rat incisor cervical loop and is therefore of ameloblast origin (66, 154). It expresses KLK4 and amelotonin, indicating maturation-stage ameloblast phenotype characteristics. It also expresses the tight junction proteins that have been found in maturation ameloblasts, including tight junction protein 1 (Tjp1/Zo1), claudin 1 (Cldn-1), claudin 4 (Cldn-4) and claudin 8 (Cldn-8). These tight junction proteins restrict the free movement of ions through the cell layer.

Typically, HAT-7 cells are cultured in DMEM/F12 Ham medium ('control medium') supplemented with 10% fetal bovine serum and 1% penicillin & streptomycin. For the experimental studies, HAT-7 cells are seeded onto permeable filters and fed with 'differentiation medium' which is the control medium supplemented with 1 mM $CaCl_2$ and 10^{-8} M dexamethasone. Grown on the permeable filters, the HAT-7 cells become polarized.

Using this model, Bori et al (66) reported the expression of key ion transporters in HAT-7 ameloblasts - NHE1, NBCe1, AE2, pendrin and CFTR - by immunostaining

and by quantitative polymerase chain reaction. Using microfluorometry to follow changes in intracellular pH, the functional activity of key transporters important in pH regulation was demonstrated. These studies demonstrated the polarization of the ameloblasts of which the apical side highly exhibited CO_2 permeability while the basolateral side exhibited lower CO_2 permeability and preferentially accumulated HCO_3^- ions. These were transported from the basolateral side to the apical side of the ameloblast layer. Among the studies reporting the ion transporters located on the ameloblast's membrane (89, 155, 156), this study was the first to demonstrate functional activity of the transporters in living cells and, in particular, the directional transport of HCO_3^- (Figure 8C) (66).

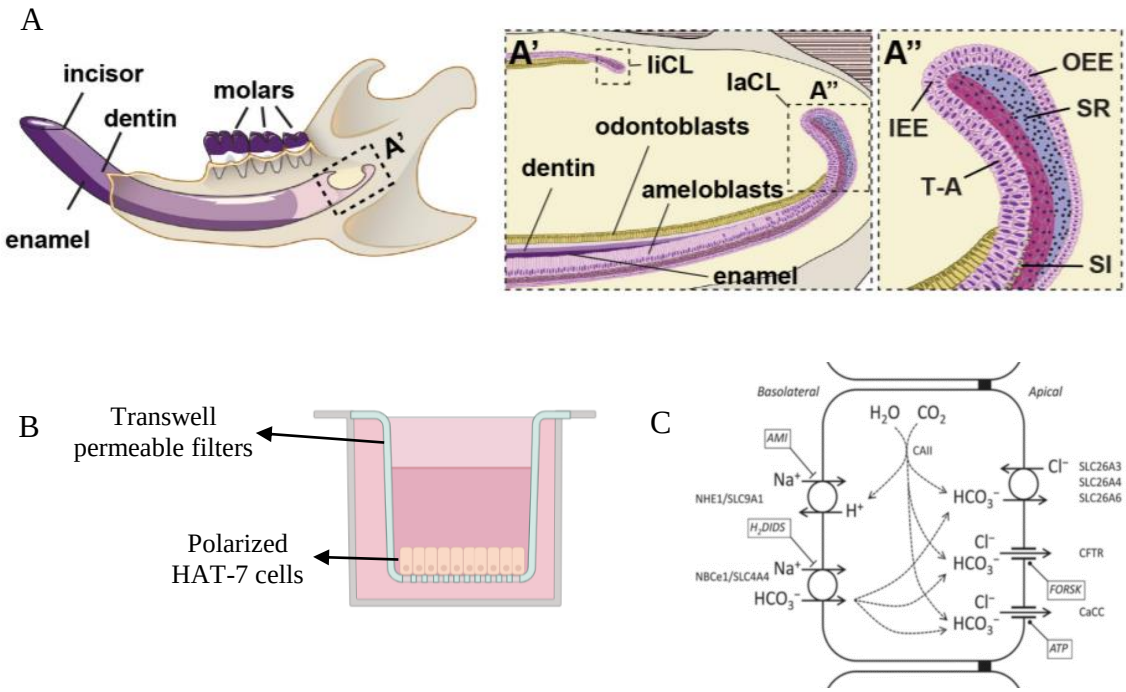

Figure 8. *Anatomical location of rodent cervical loop epithelial cells (A) and the application of HAT-7 cells for functional studies (B, C). A, structure of the rodent hemi-mandible showing the labial cervical loop (laCL in panel A') where ameloblast progenitors reside, and which is the origin of the HAT-7 cell line. B, HAT-7 cells cultured on Transwell permeable filters form a polarized monolayer. C, the proposed mechanism of vectorial HCO_3^- secretion by HAT-7 cells. Figure 8A and 8C are adapted from (Bori et al., 2016) (66), and Figure 8B is adapted from "Cell culture", by BioRender.com (2021). Retrieved from https://app.biorender.com/biorender-templates. (4)*

In 2017, Rácz et al. (67) used this model to investigate the effects of fluoride on HCO_3^- transport in the polarized HAT-7 model. In addition to confirming the localization and activity of the transporters previously reported, they demonstrated the activity of the Na^+-K^+-$2Cl^-$ (NKCC1) cotransporter located on the basolateral membrane. The fluoride studies showed that fluoride had no effect on bicarbonate transport but rather delayed the formation of the tight junctions. This 2D model is evidently suitable for investigating the functional activity of ion transporters and the disease mechanism of enamel defects such as fluorosis (66, 67).

DOI:10.14753/SE.2022.2709

2. Objectives

1. To characterize the morphology of dental stem cells and HAT-7 ameloblast-like cells cultured by conventional 2D cell culture techniques.

2. To develop a 3D ameloblast model using HAT-7 cells grown in a Matrigel matrix and to evaluate three different culture media for their potential to allow spheroid formation.

3. To inspect the histological morphology of the spheroids by cryosection and staining with hematoxylin and eosin (H&E).

4. To investigate the gene expression of the maturation-stage ameloblast marker KLK4, the tight junction proteins cldn-1, cldn-4, cldn-8 and TJP1/ZO-1, and the electrolyte transporters involved in pH regulation for comparison with the previous 2D ameloblast model.

5. To functionally examine the activity of the electrolyte transporters regulating intracellular pH in 3D HAT-7 spheroids by microfluorometry.

6. To test the toxicity of a range of fluoride concentrations on the 3D ameloblast model.

DOI:10.14753/SE.2022.2709

3. Results

3.1 Morphology of human dental mesenchymal stem cells and rat HAT-7 cell line

This study was conducted following the approval by the Semmelweis University Regional and Institutional Committee of Science and Research Ethics (17458/2012/EKU and 25459/2019/EKU). DPSCs, PDLSCs and DFSCs were isolated from human impacted wisdom teeth and residual dental follicles. At the time of seeding, these stem cells were spherical. After attachment the cells became elongated and flattened, and showed a spindle or fibroblast-like shape (Figure 9A-C). They retained this morphology and proliferated until confluence was reached. The viability of dental stem cells was measured using the WST assay to detect mitochondrial dehydrogenase activity. The number of viable cells, of all three stem cell types, cultured in both control and differentiation media, increased continuously. Hence the dental stem cells maintained the cell viability although the cell density was high (Figure 10).

HAT-7 cells were thawed from a frozen cell stock. At the time of cell seeding, the cells had a spherical shape. After a few days, the cells showed a fairly uniform polygonal shape with distinct cell borders giving a cobblestone appearance typical of epithelial cells (Figure 9D). When HAT-7 cells were grown on permeable Transwell supports, their appearance was similar to HAT-7 cells grown in plastic flasks, and the outlines of the 0.4 μm pores in the Transwell supports can also be seen (Figure 9E).

DOI:10.14753/SE.2022.2709

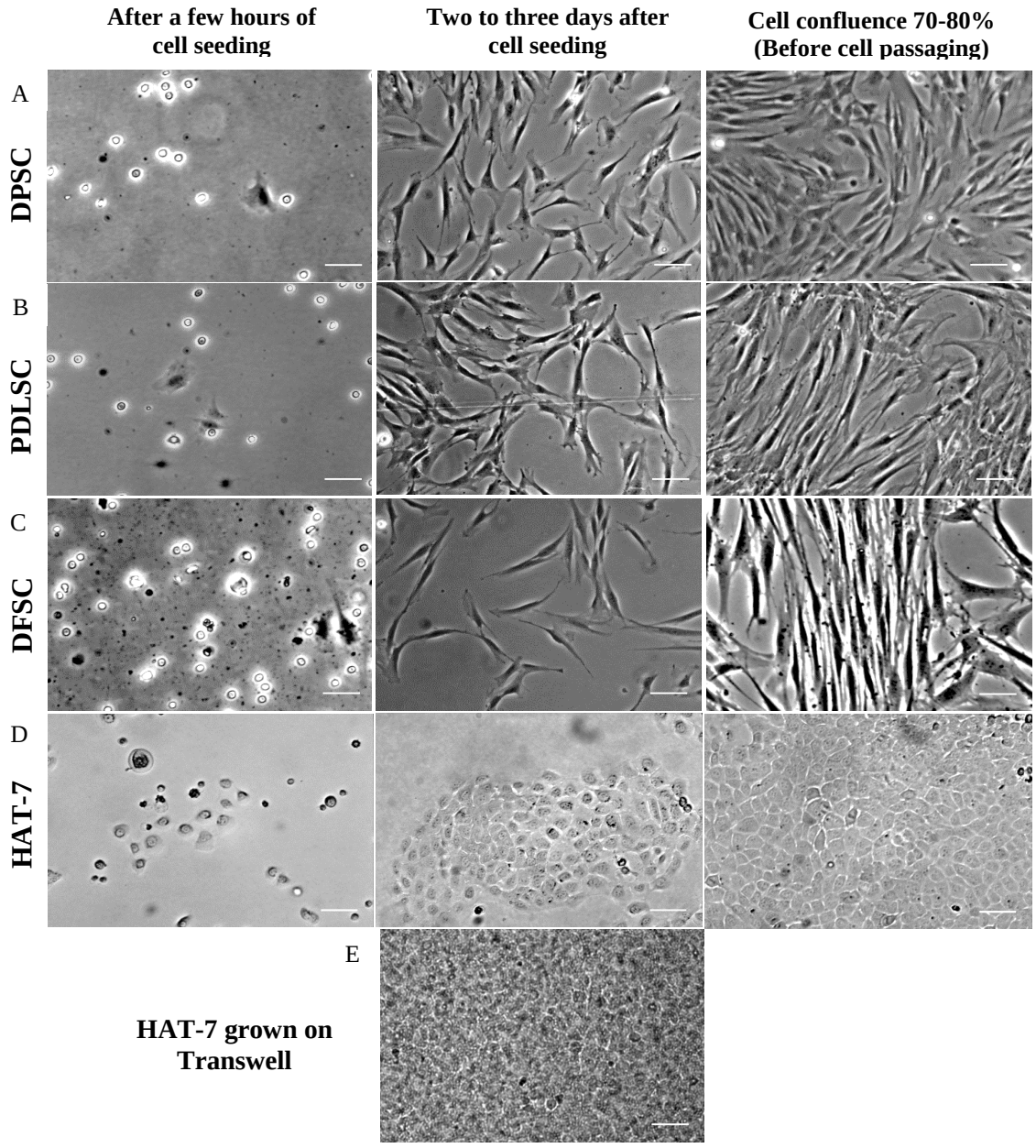

Figure 9. *The fibroblast-liked appearance of primary dental stem cells: human dental pulp stem cells (hDPSC) (A), human periodontal ligament stem cells (hPDLSC) (B), and human dental follicle stem cells (hDFSC) (C) and the cobblestone appearance of HAT-7 cells (D) cultured in control medium, after a few hours of cell seeding, three days of culture, and before the cell passaging. (E) The morphology of HAT-7 cells grown on a Transwell support in differentiation medium once confluence had been reached. Scale bars: 50 μm.*

DOI:10.14753/SE.2022.2709

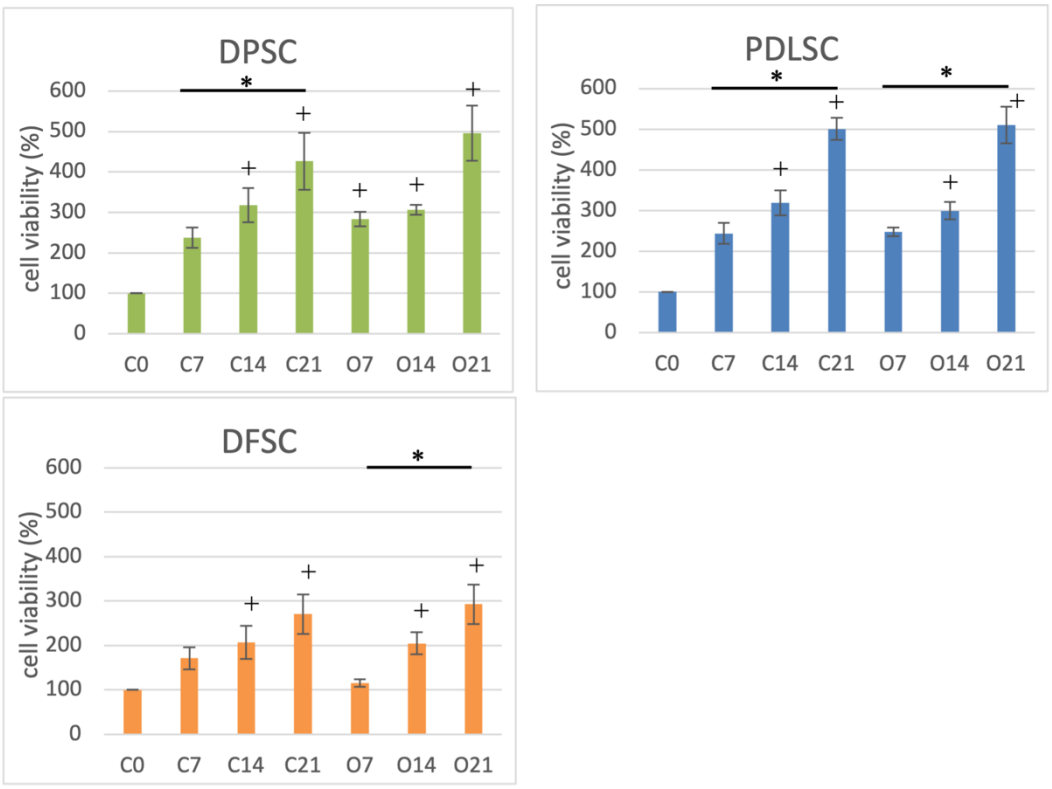

Figure 10. *Numbers of viable cells in cultures of three different stem cells originated from dental tissues: dental pulp stem cells (DPSCs), periodontal ligament stem cells (PDLSCs), and dental follicle stem cells (DFSCs) cultured in control (C) or osteogenic (O) medium for three weeks. The numbers on the x-axis indicate the day of culture. The data were normalized to day 0.*

3.2 3D culture of HAT-7 cells with basement membrane matrix

Suspended single HAT-7 cells in three different media (control, differentiation, and Hepato-STIM) were mixed with Matrigel matrix and seeded in low-attachment plate wells. Spheroid development was monitored over a period of two weeks. Figure 11A shows the morphology of the cells/spheroids at the beginning, and after three days, one week and two weeks of culture. Initially, the cells in different three culture media were relatively uniform and similar in size, approximately 20 μm in diameter. After three days of cell seeding, the size and appearance of the cells had changed only slightly. But after a week, some of the cells cultured in control and differentiation medium showed signs of division. And after two weeks, most of the cells retained a similar size and appearance as

at the beginning. Only a few had become larger and developed into multicellular spheroids.

On the other hand, the cells incubated in Hepato-STIM medium proliferated and developed a multicellular spherical appearance much more quickly and persistently after three days of culture. Within one week, many spheroids, which were approximately 100 μm in diameter, had developed. When the culture was continued, the spheroids had become huge and begun to disintegrate.

A remarkable difference in the size of the cells/spheroids developed in the three different media was initially observed on day 4 and this is compared on days 4-6 in Figure 11B. The median area of the cells/spheroids cultured in the control and differentiation medium was around 1000 μm^2 and the area hardly increased on days 5 and 6. The median size of the cells/spheroids cultured in Hepato-STIM was about 2500 μm^2 and they almost doubled in area over the next two days. This explicitly indicates the faster growth of the spheroids in Hepato-STIM compared to the other two media. Moreover, the number and size of the spheroids produced in Hepato-STIM were significantly greater than in the other two media, even when the cells in the control and differentiation medium were cultured for more than two weeks.

Based on these results, spheroids grown for one week in Hepato-STIM were used for subsequent experiments examining protein expression and functional activity.

DOI:10.14753/SE.2022.2709

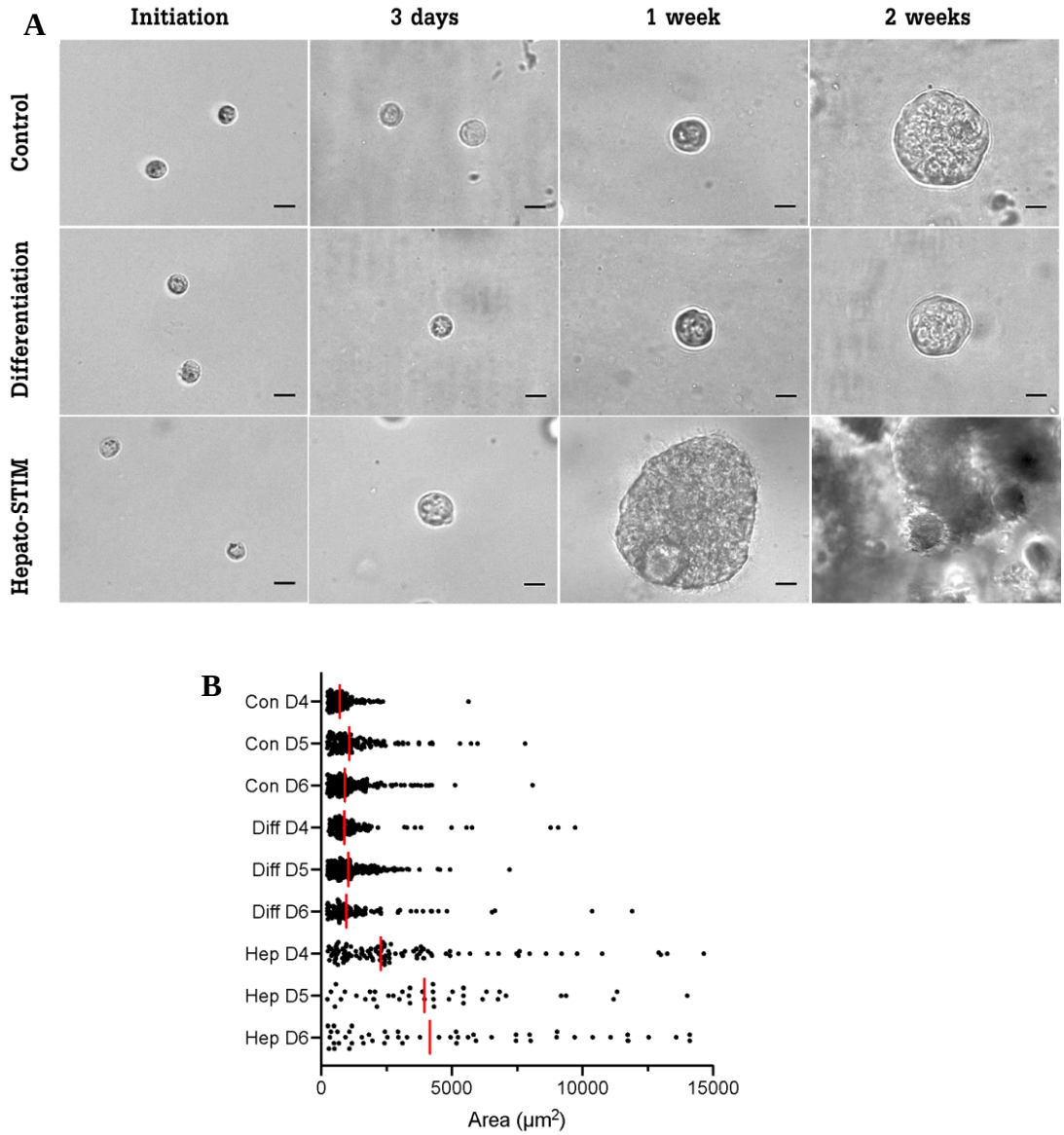

Figure 11. *HAT-7 spheroid development in Matrigel matrix. (A) Morphology of HAT-7 cells cultured with three different culture media: control, differentiation, and Hepato-STIM. The growth and spheroid development of HAT-7 cells in each medium was displayed on the day of seeding, and after 3 days, 1 week and 2 weeks. (B) The diverse size of HAT-7 cells/spheroids incubated in three different culture media was compared on days 4, 5 and 6 (D4-D6). Each black dot represents the area of a single cell/spheroid. The vertical red bars represent the median values. Scale bars: 20 µm.*

DOI:10.14753/SE.2022.2709

3.3 Histological morphology

Histological examination of the HAT-7 spheroids, cultured in Matrigel matrix with Hepato-STIM medium for seven days, was performed using frozen sections stained with hematoxylin and eosin. The morphology of the spheroids varied considerably (Figure 12). The smallest spheroid was around 70 μm in diameter. Its structure was the least complicated, and it contained a dense aggregation of undifferentiated cells with randomly distributed small pools of extracellular fluid or ‘lacunae’ (Figure 12A). The intermediate sized spheroids were around 100 μm in diameter. They contained significant numbers of lacunae and presented an emerging outer epithelial layer connected in several places to the central cell mass (Figures 12B–D). The largest spheroids exhibited an outer epithelial monolayer wholly separated from a central cell mass by a clear fluid-filled space or lumen (Figures 12E–H). The central cell mass was either disorganized and undifferentiated (Figures 12E, F) or had a lamellar structure (Figures 12G, H).

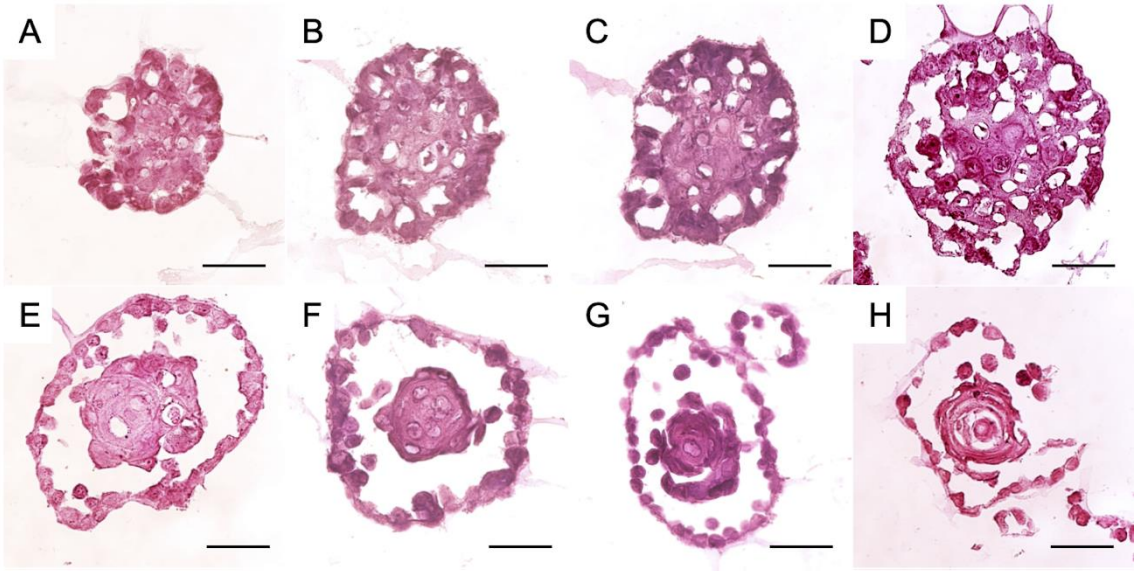

Figure 12. *Morphology of HAT-7 spheroids cultured in Matrigel matrix with Hepato-STIM medium for seven days. Spheroids were released from the matrix and processed for cryosection. The sections were cut at 5-μm thickness and stained with hematoxylin and eosin. Scale bars: 50 μm.*

3.4 Gene expression of ameloblast markers, tight junction proteins and transporters

Expression levels of the genes of interest were examined by quantitative RT-PCR to determine their relative mRNA levels. RNA was extracted from HAT-7 spheroids grown in Matrigel matrix with Hepato-STIM medium for a week (our preferred model) and from HAT-7 monolayers grown on Transwell permeable supports as obtained for previously published functional studies (66, 67). Data from both sample groups were compared to detect any significant differences in gene expression level between the previous 2D cultures and this 3D HAT-7 cell model (Figure 13). The highest expression level among the chosen genes was KLK4, a maturation-stage ameloblast marker. The expression level of KLK4 in the spheroids was approximately 70-fold greater than in the 2D HAT-7 model (Figure 13A). Of the four tight-junction proteins examined, only cldn-8 was significantly increased in HAT-7 spheroids compared to the 2D model. Expression levels of the other three, cldn-1, cldn-4 and TJP1/ZO-1, were significantly decreased in the spheroids compared to the 2D model (Figure 13A). Most of the electrolyte transporters involved in HCO_3^- secretion by maturation-stage ameloblasts, SLC9A1/NHE1, SLC4A2/AE2 and SLC4A4/NBCe1, were detected in the HAT-7 spheroids but were expressed at slightly lower levels than in the 2D model (Figure 13B). Interestingly, the other two transporters, SLC26A4/pendrin, and CFTR, generally located on the apical membrane, were significantly reduce in the spheroids compared to the 2D model.

DOI:10.14753/SE.2022.2709

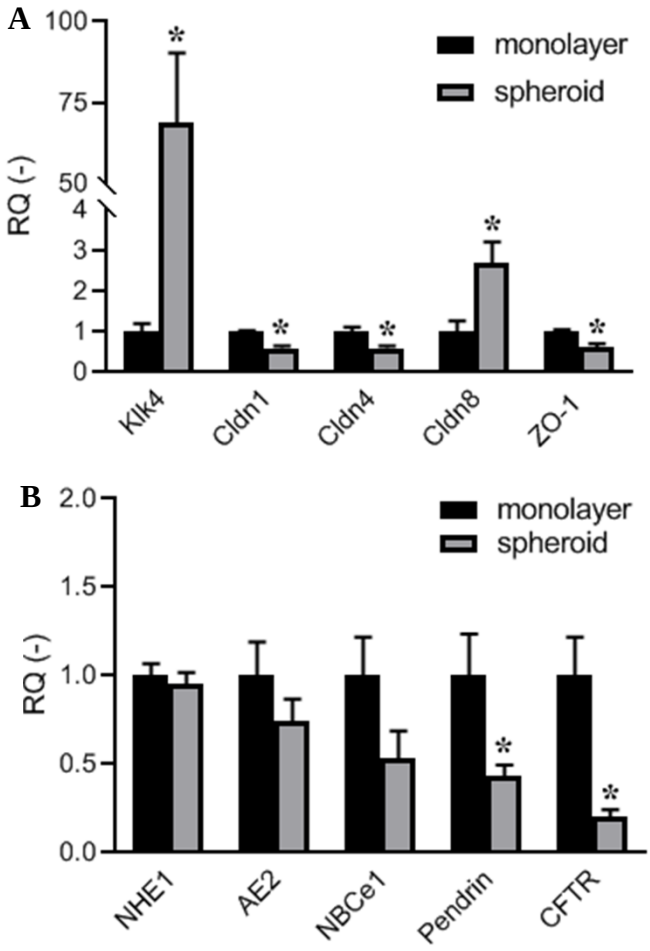

Figure 13. *Quantitative RT-PCR data indicating gene expression levels in HAT-7 spheroids cultured in Matrigel matrix with Hepato-STIM medium for seven days, normalized to the corresponding 2D monolayer culture data. (A) expression of the maturation-stage ameloblast marker gene KLK4 and the tight-junction protein genes, cldn-1, cldn-4, cldn-8 and Tjp1 (ZO-1). (B) expression of electrolyte transporter genes Slc9a1 (NHE1), Slc4a2 (AE2), Slc4a4 (NBCe1), Slc26a4 (pendrin) and Cftr (CFTR). Data presented as mean ± SEM. *p < 0.05 (n = 4).*

3.5 Intracellular pH regulation

Previous studies have identified some of the electrolyte transporters located on the apical and basolateral membranes of HAT-7 cells (66, 67). These transporters play an essential role in neutralizing protons during crystal formation in the enamel. In this study, the same standard protocol was used to assess the activity of each transporter in HAT-7 spheroids. Spheroids grown in Matrigel matrix with Hepato-STIM medium for seven days were

DOI:10.14753/SE.2022.2709

isolated and plated on coverslips coated with 0.01% poly-L-lysine (Figure 14). The spheroid cells were loaded with the pH-sensitive fluorescent dye BCECF and the changes in intracellular pH measured by microfluorometry.

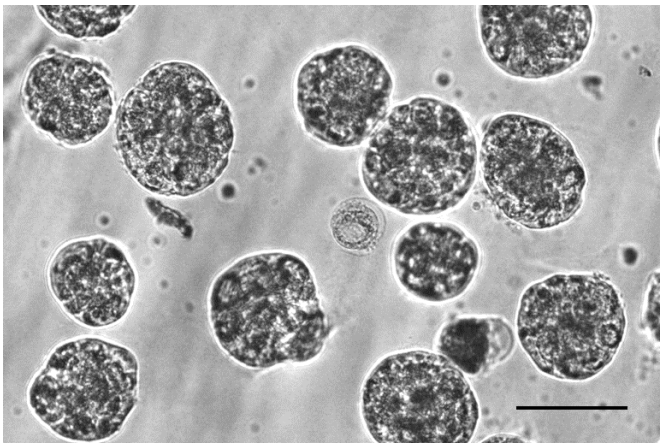

Figure 14. *HAT-7 spheroids cultured in the Matrigel matrix with Hepato-STIM for seven days were isolated and plated on coverslips for microfluorometry experiments. Scale bar: 75 μm.*

3.5.1 Na^+-H^+ Exchanger

To assess Na^+-H^+ exchanger activity in the spheroid cells, the rate of pH_i recovery from the acid loading induced by exposure to an ammonium pulse was measured in a HCO_3^--free, HEPES-buffered physiological salt solution. HAT-7 spheroids were exposed to 20 mM NH_4Cl for 3 minutes resulting in a transient alkalinization of the cells before a quick, rapid drop in pH_i to a markedly acidic value (Figure 15A). This intracellular acidification was sustained in the absence of Na^+ by substitution of extracellular Na^+ with $NMDG^+$. This showed that the cells were unable to extrude H^+ from the cells without Na^+. In other words, the spheroid cells have no Na^+-independent pathway for extruding H^+, such as an H^+-ATPase. When Na^+ was restored, pH_i quickly recovered to control values. This indicates Na^+ is required to extrude H^+, so there might be a Na^+-dependent H^+ extruder in HAT-7 spheroids. This was confirmed by repeating the procedure and restoring Na^+ in the presence of a selective inhibitor of Na^+/H^+ exchanger, amiloride (0.3 mM). The rate of pH_i recovery from acidification was greatly decreased (Figure 15D). Thus, an Na^+/H^+

exchanger, most likely to be NHE1, exists in HAT-7 spheroids. The average percentage inhibition of the pH_i recovery rate, compared to the control, is shown in Figure 15D.

3.5.2 Na^+-HCO_3^- Cotransporter

To assess the activity of Na^+-HCO_3^- cotransporters in the spheroids, the above process was repeated, but this time in a bath solution containing HCO_3^-. When Na^+ was restored after the intracellular acidification in the presence of amiloride, the recovery from acidification was not completely inhibited by amiloride (Figures 15B, D). This HCO_3^-- and Na^+-dependent component of the recovery from acidification is most likely due to a HCO_3^-- and Na^+-dependent transporter such as an Na^+-HCO_3^- cotransporter. When Na^+ was restored in the presence of both amiloride and H_2DIDS (0.5 mM) - an inhibitor of Na^+-HCO_3^- cotransport - the inhibition of pH_i recovery was more potent than that due to amiloride alone (Figures 15C, D). This suggests that a Na^+-HCO_3^- cotransporter, most likely to be NBCe1, is active in HAT-7 spheroids.

3.5.3 Cl^--HCO_3^- Exchanger

To assess the activity of anion exchangers in HAT-7 spheroid cells, extracellular Cl^- in the HCO_3^--buffered bath solution was substituted with gluconate and the resulting changes in pH_i were measured. Extracellular Cl^- withdrawal reverses the existing concentration gradient of Cl^-, which would result in Cl^- efflux from the cells driving an influx of HCO_3^-, and a rise in pHi, if anion exchangers were active in the HAT-7 spheroid cells. As expected, a notable increase in pH_i in the spheroid cells could be detected (Figure 15E). When Cl^- was restored to the bath solution, pH_i returned to the normal value. When the experiment was repeated in the presence of 0.1 mM DIDS, an inhibitor of Cl^-/HCO_3^- exchange, the rate of change in pH_i was clearly reduced. This suggests the presence of an active Cl^-/HCO_3^- exchanger, most probably AE2, in HAT-7 spheroids.

DOI:10.14753/SE.2022.2709

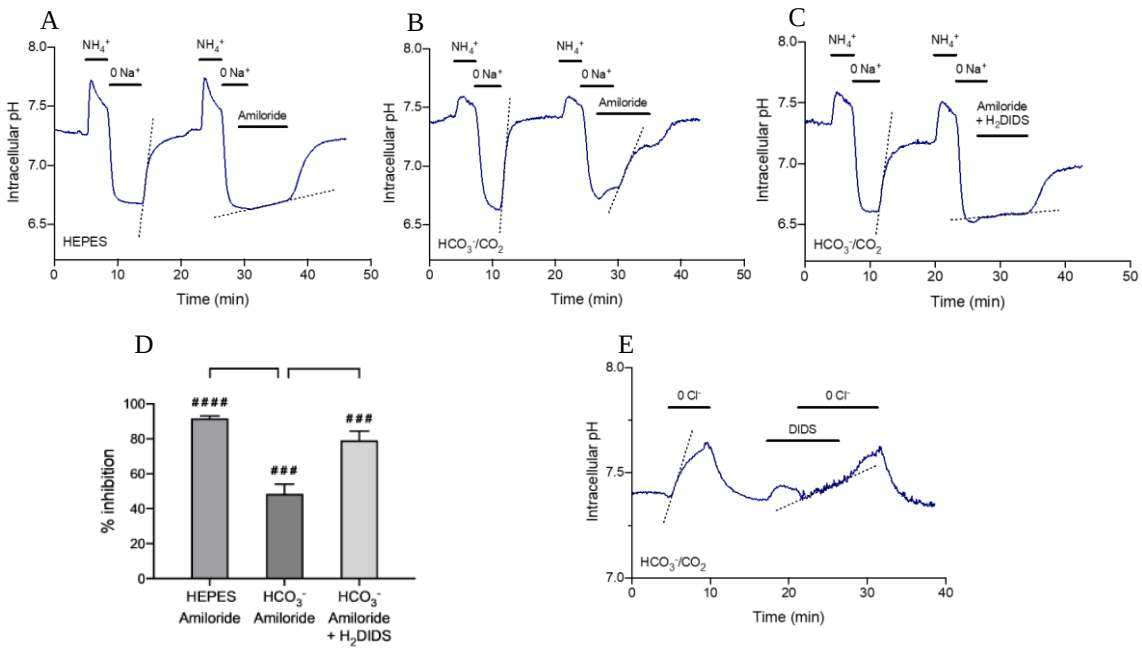

Figure 15. *Changes in pH_i of HAT-7 spheroids measured by microfluorimetry. (A-C) Recovery of pH_i from intracellular acidification. The spheroids were exposed to 20 mM NH_4^+ for 3 minutes, followed by extracellular Na^+ withdrawal by replacement with $NMDG^+$ (0 Na^+): (A) in HEPES-buffered bath solution with and without 0.3 mM amiloride; (B) in HCO_3^--buffered bath solution with and without 0.3 mM amiloride; (C) in HCO_3^--buffered bath solution with or without a combination of 0.3 mM amiloride and 0.5 mM H_2DIDS. (D) The average percentage inhibition of pHi recovery rate in the presence of amiloride with or without H_2DIDS and with or without HCO_3^-. Mean (± SEM) calculated from 4-6 experiments with reference to the internal control in each experiment. ####p < 0.0001, ###p < 0.001 compared with control (one-sample t-test). (E) The increase in pH_i induced by substituting extracellular Cl^- with gluconate (0Cl^-) in a HCO_3^--buffered bath solution with or without 0.1 mM DIDS. The rates of change of pH_i when Na^+ was restored (A-C) or Cl^- removed (E) are shown as dashed lines.*

3.6 Fluoride exposure

An experiment to investigate the effect of fluoride on HAT-7 spheroids was divided into two series depending on when the HAT-7 cells/spheroids cultured in Matrigel matrix were first exposed to fluoride. Both series comprised a control group that was not exposed to fluoride and an experimental group exposed to a range of fluoride concentrations: 0.1,

0.3, 1.0 and 3.0 mM. In the first series, fluoride was added to the medium after 24 hours when the cells were already embedded in the Matrigel matrix. Images of spheroid formation on day 2 and 7 of culture and of the spheroids after isolation from the matrix on day 7 are shown in Figure 16A. The HAT-7 cells grew and formed spheroids quickly and uniformly in the control group, as described in section 3.2 (Figure 11A). HAT-7 cells exposed to 0.1 and 0.3 mM fluoride were also able to form spheroids that were similar in size and appearance to the control group. On day 7, spheroids released from the matrix also retained the same size and appearance as the control group. Therefore, 0.1 and 0.3 mM fluoride did not visibly affect cell proliferation and spheroid formation. In the 1 mM fluoride medium, however, only a few HAT-7 cells were able to develop into spheroids, and the size of these spheroids was smaller than those in the control group or lower fluoride concentration groups. A large number of cells died and were seen as cellular debris. On day 7, those few spheroids that were released from the matrix remained smaller than the control group. Only a few HAT-7 cells exposed to 3 mM fluoride survived, and no spheroids developed.

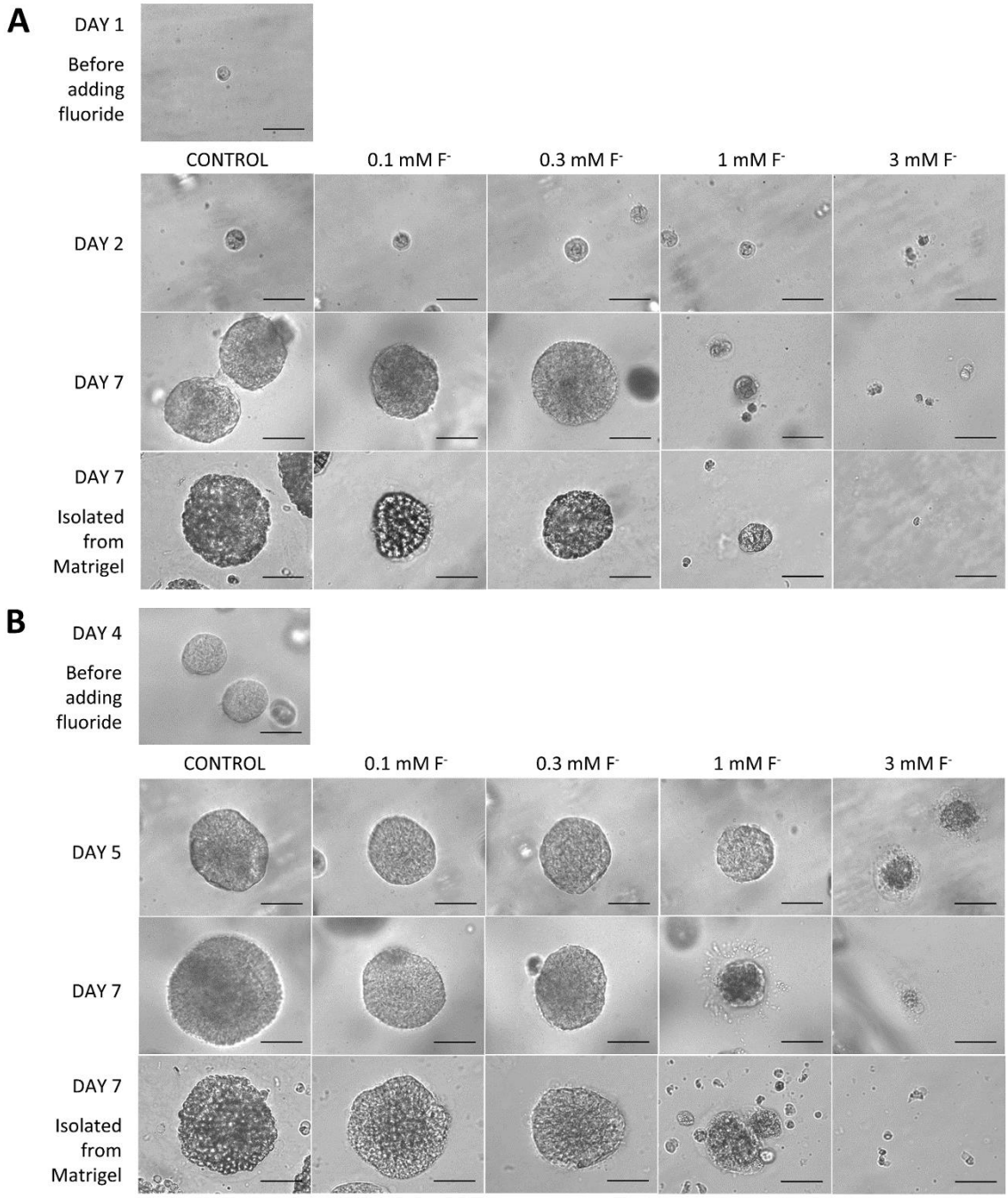

Figure 16. *Morphology of HAT-7 spheroids cultured in Matrigel matrix with Hepato-STIM medium containing 0 mM (control), 0.1, 0.3, 1 and 3 mM fluoride. (A) Spheroid appearance on days 1, 2 and 7 when the fluoride was introduced 24 hours after cell embedding in the matrix. (B) Spheroid appearance on days 4, 5 and 7 when fluoride was introduced on day 4 after the spheroids had already formed. The appearance of spheroids isolated from the matrix on day 7 is also shown. Scale bars: 70 μm.*

In the second series, fluoride was introduced on day 4 when the HAT-7 cells had already established a multicellular spherical appearance and had started enlarging rapidly (Figure 16B). HAT-7 spheroids exposed to 0.1 and 0.3 mM fluoride retained their ability to proliferate and the spheroids grew in size. The size and number of the spheroids, including their growth rate, were similar to those grown in the control medium. Thus again, 0.1 and 0.3 mM fluoride had little or no effect on the growth of the spheroids. As in the first series of experiments, the higher fluoride concentrations (1 mM and 3 mM), when introduced on day 4, more visibly affect spheroid growth. In the presence of 1 mM fluoride, the existing spheroids gradually decreased in size and were disaggregating by day 7. This effect was also noticeable when the spheroids were isolated from the matrix. Only a few intact spheroids were seen while a lot of cell debris was present. This was also observed in the spheroids exposed to 3 mM fluoride, but the death and disintegration of the spheroids developed more quickly, and no spheroids were seen by day 7.

4. Discussion

The present study successfully establishes a 3D ameloblast model retaining several of the characteristics and functions of maturation-stage amelogenesis in more physiological representation of the *in vivo* environment. Spheroids were obtained by growing dissociated HAT-7 cells in Matrigel matrix with Hepato-STIM medium. These conditions supported cell proliferation, spherical structure formation and differentiation. HAT-7 cells in spheroids showed a polarized epithelial cell appearance and the expression of ameloblast-specific markers and electrolyte transporters at the mRNA level. HAT-7 spheroids also functionally regulated their intracellular pH. Experiments exploring the toxicity of fluoride showed the potential of HAT-7 spheroids for use as an in vitro disease model.

In tissue engineering, the fundamental components - cells, a scaffold and bioreactive molecules - can work together to regenerate tissues or organs (157). Similarly, to establish an experimental model for amelogenesis, cells selection should be carefully considered. In conventional (2D) cell culture of cells derived from dental tissues, DFSCs, PDLSCs and DPSCs established a non-epithelial morphology, with spindle-shaped, fibroblast-like cells. These are all mesenchymal stem cells that possess multipotent differentiation capacity (119, 139, 158). They are of neural crest origin (127) and are able to maintain their viability in an osteogenic medium for three weeks and have osteogenic differentiation capacities. They can also differentiate into odontoblast, myoblasts, neural cells, adipocytes and endothelial cells (127, 137-139). However, no evidence of the differentiation of dental stem cells to ameloblast cells has been found. The HAT-7 cell line, on the other hand, exhibits epithelial characteristics and expresses KLK4 and amelotonin, which are markers for maturation-stage ameloblasts (66, 67, 154). Therefore these cells have become widely adopted for amelogenesis research and the present study has shown their potential for establishing a 3D functional ameloblast model.

Apart from cell selection, it was necessary to identify the best conditions for growing HAT-7 cells in the Matrigel matrix. The cells were initially cultured in three different media, control, differentiation, and Hepato-STIM medium, following our previous work to develop a functional 2D HAT-7 cell model (66). Differentiation medium was found to be suitable for HAT-7 cells cultured on Transwell membranes (66, 67). However, the differentiation medium seemed to be inappropriate for HAT-7 cells grown

in Matrigel matrix. The use of Hepato-STIM, rather than the other two media, yielded larger sizes and larger numbers of HAT-7 spheroids. Hepato-STIM medium is a commercially available epithelial selection medium, originally developed for hepatocyte culture; however, it has been used for growing other epithelial cells, e.g., human primary salivary epithelial cells (151, 159, 160) and lacrimal acinar cells (161, 162). Hepato-STIM can support the growth of epithelial cells because its components (Williams' E medium, dexamethasone, insulin, transferrin, selenium, EGF and 1.8 mM Ca^{2+}) contribute to maintaining an epithelial phenotype (151, 159, 160).

To develop HAT-7 spheroids, the Matrigel matrix was selected as a scaffold due to its capacity for enabling cell morphogenesis and differentiation. Additionally, it is known to support spheroid or organoid culture from various cell and tissue types (151, 160, 163-165). Matrigel matrix is a solubilized basement membrane extract derived from the Engelbreth-Holm-Swarm (EHS) mouse tumor. The matrix contains anchoring molecules with arg-gly-asp (RGD) sequences, supports cell adhesion, and crucial extracellular substances, such as laminin-111, that offer biological signals for spheroid or organoid development and growth. Its stiffness is optimal for housing cells (166) and is loose enough to enable spheroids/organoids to develop and grow. Matrigel supports the development of 3D structures from pancreas (167, 168), intestinal epithelium (163, 164), lacrimal glands (161, 165), salivary glands (151, 160, 169) and ameloblast lineage cells (170, 171).

Epithelial cells cultured in 3D extracellular matrices, such as Matrigel, can polarize and generate lumen-containing spherical structures imitating the *in vivo* structure of tissues (172, 173). Epithelial cells forming cysts or lumens in 3D culture all become polarized so that the apical membrane faces toward the lumen while the basal side contacts the matrix (148, 173, 174). We believe this is also true for the HAT-7 cells in the lumen-containing spheroids.

Some research showed the 3D ameloblast spheroids developed by culturing primary ameloblast lineage cells in Matrigel (170, 171, 175). Epithelial cells isolated from the porcine enamel organ and the cervical loop of mouse incisor are known to proliferate and form epithelial pearl-like structures in Matrigel (170, 171). These structures also express the ameloblast markers amelogenin, MMP-20 and KLK4. Additionally, two studies have reported the differentiation of ameloblast cells from human embryonic stem cell lines

grown on Matrigel matrix and co-cultured with dental mesenchymal cells (176, 177). These cells were even able to form tooth-like structures. Previous research shows that primary or secondary ameloblast-lineage cells can form spherical structures when cultured in or on Matrigel matrix much like the 3D HAT-7 spheroids generated in the present study.

Gene expression at the mRNA level in HAT-7 spheroids cultured in Matrigel matrix and Hepato-STIM medium was investigated and compared to HAT-7 cells grown on Transwell permeable supports. The significantly higher expression of KLK4 in HAT-7 spheroids, compared to HAT-7 cells grown on Transwells, suggests a greater differentiation towards the maturation-ameloblast phenotype. KLK4 is the proteolytic enzyme dominantly observed in the maturation stage and needed to degrade the enamel proteins, which is a prerequisite for mineral deposition (21, 84). The HAT-7 spheroids also formed mature tight junctions as detected by mRNA expression of the key tight junction proteins. Tight junction formation is a prerequisite for limiting the free transepithelial movement of solutes and for allowing the vectorial transport of specific ions (178, 179). HAT-7 spheroids showed expression of the tight junction proteins cldn-1, cldn-4, cldn-8 and Zo-1, consistent with other studies (66, 67, 178, 179). Interestingly, the expression of cldn-1, cldn-4 and Zo-1 was significantly lower than in HAT-7 cells grown on Transwells. On the other hand, the expression of cldn-8 was significantly higher than in HAT-7 cells grown on Transwells (66). The increased expression of cldn-8 in the spheroids may raise paracellular leakage (180).

The role of ameloblasts in regulating pH during the maturation stage of amelogenesis has been examined by both the molecular and functional approaches. Key acid/base transporters, such as NHE1, AE2, NBCe1, pendrin and CFTR, have been reported (21, 84, 89, 181). These were also detected in the HAT-7 spheroids by quantitative RT-PCR although their expression levels were generally lower than in HAT-7 cells grown on Transwells. Interestingly, the expression of two transporters generally located at the apical membrane, pendrin and CFTR, was significantly decreased in the spheroids compared with HAT-7 cells grown on Transwells. This is consistent with our previous finding (66), that HAT-7 cells grown in hepato-STIM medium in 2D culture have reduced expression of acid/base transporters. The apparent reduction in tight junction protein and electrolyte transporter expression in HAT-7 spheroids may be due to

the diluting effect of mRNA from the relatively undifferentiated cells in the central cell mass of the spheroid. Nevertheless, the reduced expression of both tight junction proteins and electrolyte transporters in HAT-7 spheroids did not affect their ability to regulate intracellular pH.

A mechanism for the neutralization of H^+ ions liberated during Hap crystal formation has been proposed on the basis of data obtained from the 2D ameloblast model (66, 67). HAT-7 cells grown on permeable supports express several acid/base transporters involving pH regulation and bicarbonate secretion. A function of the transporters located on the basolateral membrane is to take up HCO_3^- for secretion by acid/base transporters at the apical membrane (66, 67). pH_i regulation by ameloblast following the introduction of NH_4^+ has helped to identify the possible mechanism and transporters. The transporter that primarily contributes to HCO_3^- uptake at the basolateral side is inhibited by H_2DIDS, suggesting that it is an Na^+-HCO_3^- cotransporter (NBCe1). HCO_3^- uptake is also indirectly achieved by H^+ extrusion through an amiloride-sensitive Na^+/H^+ exchanger (NHE1). This NHE1 extrudes the H^+ ions resulting from intracellular carbonic anhydrase activity, which continuously generates H^+ and HCO_3^- from CO_2 and water. pH_i measurements in HAT-7 spheroids confirm the presence of active acid/base transporters similar to those observed in HAT-7 cells grown on permeable supports. There was no evidence of any basolateral H^+-ATPase involvement in the uptake of HCO_3^- ions. However, the activity of a Cl^-/HCO_3^- exchanger, most probably AE2, was detected in HAT-7 spheroids during Cl^- substitution experiments combining with DIDS inhibition. This anion exchanger contributes to basolateral uptake of Cl^- ions, which are also required for enamel formation (84, 181). The development of this 3D ameloblast model should enable further studies of ameloblast-mediated ion transport and enamel mineralization in a more physiological experimental preparation.

The significant decrease in CFTR expression in HAT-7 spheroids was concerning. *In vivo*, CFTR is highly expressed in maturation-stage ameloblasts after its low level of expression in the transition stage and almost complete absence in the secretory stage (89, 181). One previous study cultured primary ameloblast-derived cells in Matrigel matrix and found increased expression of amelogenin (175). Amelogenin is notably expressed in secretory-stage ameloblasts; therefore, ameloblast-lineage cells cultured in 3D culture systems may de-differentiate to an earlier stage of ameloblast development. This calls for

further studies investigating alternative culture media or 3D culture systems to explore the interesting alternative differentiation pathways.

Disturbances during amelogenesis, such as excessive amounts of fluoride, can seriously affect the characteristics and properties of mature enamel (9, 89, 104). The 3D HAT-7 model was tested with various concentrations of fluoride ranging from 0.1-3 mM. The lower concentrations of fluoride (0.1 and 0.3 mM) did not affect spheroid formation. In contrast, all HAT-7 cells died within two days when exposed to 3 mM fluoride. When 1 mM fluoride was applied after 24 hours of seeding cells in the Matrigel matrix, the spheroids could develop, but their size and number were smaller than the control. When 1 mM fluoride was applied after day 4 of cell culture, the spheroid size gradually decreased. They were disaggregating by day 7, resulting in a few remaining, small-sized spheroids and significant amounts of cell debris.

Exposure to the lower concentrations of fluoride (0.1 and 0.3 mM) for three or even six days did not affect the process of spheroid formation, and spheroid yields were comparable to the control group. According to recent research (67), low concentrations of fluoride applied to the 2D HAT-7 model similarly had no effect on HAT-7 monolayer growth on permeable supports. Spheroids exposed to 1 mM disintegrated after being gently isolated from the Matrigel matrix, suggesting that 1 mM fluoride disrupts spheroid formation by impairing cell-cell adhesion. This is in line with the reported effect of fluoride delaying tight junction formation in the 2D HAT-7 model (67).

The death of HAT-7 cells/spheroids caused by exposure to 3 mM fluoride might be explained by the inhibition of antioxidant enzyme activity, leading to excessive free radicals (ROS), which damage intracellular organelles and cell membranes. Moreover, the processes of cell death such as apoptosis can also be activated (108-113, 182).

Studies of the effects of micromolar fluoride on ameloblast cell cultures, both primary cells and cell lines, have found very little to no changes in gene expression, although effects on cell proliferation and apoptosis are observed (107, 111, 153, 183-185). The effects of fluoride on 3D HAT-7 spheroids suggest that they depend on the fluoride concentration as observed previously (26, 105).

Limitations of the study

The concepts behind the previous 2D HAT-7 cell model and the new 3D model are based on culturing ameloblast-liked cells on something similar to a basement

membrane. Both the Transwells used for 2D culture and the Matrigel matrix used for 3D culture allow the cells to adhere to a permeable surface and become polarized. The 2D ameloblast model works well for determining the direction and mechanism of HCO_3^- secretion for pH regulation during amelogenesis. It has clearly demonstrated that HCO_3^- ions are taken up by basolateral transporters and secreted by apical transporters (66, 67). This model is easy to produce and consumes less time than 3D cell culture. However, the 2D model does not mimic the true, physiological environment in vivo and is not suitable for developing cell-based therapies or for use in tissue regeneration (8). This is why the 3D ameloblast model was established in order to culture ameloblast-like cells in an environment more closely resembling the *in vivo* condition. This 3D ameloblast model shows the potential for more complete differentiation of the HAT-7 cells towards the maturation-stage ameloblast phenotype. It also expresses the acid/base transporters required for pHi regulation and, by extension, the potential for neutralizing the excess H^+ ions in the enamel space during crystallization. On the other hand, without further development, it would be technically difficult to investigate vectorial ion transport in this model.

The 3D culture technique is also sensitive to changes in the composition of the Matrigel matrix, which is a natural extract whose protein concentration and other components vary between batches (8, 149). And because this matrix is isolated from mouse sarcoma, its application to tissue regeneration is limited to animal studies. At present, the size of the spheroids is uncontrollable, and their use with other scientific methods requires additional isolation steps (8, 148). In addition, the cost-effectiveness of these methods must be considered (8).

Finally, it has to be noted that this 3D ameloblast model is a homotypic spheroid composed of a single cell type. Full differentiation of functional ameloblasts capable of enamel formation probably requires induction by adjacent mesenchymal cells. Consequently, this 3D ameloblast model requires further development before it becomes suitable for use in tissue repair and tooth regeneration.

5. Conclusions

1) Dental stem cells and HAT-7 ameloblast-like cells established different cell morphologies *in vitro*. Dental stem cells showed a fibroblast-like appearance indicating mesenchymal characteristics. HAT-7 cells showed a polygonal, cobble-stone appearance, which is characteristic of epithelial cells.

2) In the present work, the establishment of a 3D ameloblast model has been successfully achieved by culturing HAT-7 cells in Matrigel matrix and by feeding with Hepato-STIM medium. This system enabled HAT-7 cells to form multicellular spherical structures.

3) HAT-7 spheroids showed the potential for morphogenesis by forming multicellular structures, many of which also contained a lumen.

4) HAT-7 spheroids expressed the maturation-ameloblast marker KLK4, tight junction proteins and basic electrolyte transporters. The spheroids showed evidence of differentiation towards maturation-stage ameloblasts.

5) HAT-7 spheroids demonstrated the capacity for intracellular pH regulation by the verified activity of key H^+/HCO_3^- transporters.

6) In the 3D HAT-7 model, spheroid development exhibited different outcomes depending on the extent of fluoride exposure, suggesting that the severity depends on the concentration of fluoride.

From all of the above we can conclude that this 3D HAT-7 model offers opportunities for studying maturation-stage amelogenesis in physiological conditions closer to those that exist *in vivo*. The model is not only suitable for morphological and molecular studies but also for functional investigations. Additionally, it can be used to study pathologic conditions, such as fluorosis. In summary, this new experimental model provides a basis for better understanding amelogenesis and it hints at the potential of 3D ameloblast organoids for tissue repair and/or tooth regeneration.

The highlight novel observations presented in this thesis are the following:

1) This 3D ameloblast model, established from HAT-7 cells and Matrigel matrix, is the first ameloblast study model that shows lumen formation and the functional activity of pH regulatory and HCO_3^- transport proteins.

2) This study model may be a useful alternative model for examining the mechanisms and/or results of enamel diseases such as fluorosis.

DOI:10.14753/SE.2022.2709

6. Summary

The study of amelogenesis is mainly based on histological and molecular research performed in animal models or *in vitro*. Although the mechanism of amelogenesis has been intensively studied for decades, the mechanisms are still incompletely understood. Recently, a functional 2D model was developed for studying amelogenesis *in vitro*. This used HAT-7 ameloblast-like cells, originating from the rat incisor, that were cultured on Transwell permeable filters. HAT-7 cells exhibited maturation ameloblast characteristics, formed tight junctions, and were capable of the vectorial secretion of HCO_3^-. Alghough animal models can provide information related to the real physiological environment, the use of laboratory animals in functional studies is limited by technical difficulties and by ethical concerns. To bridge the gap between 2D cell cultures and animal models, 3D cell culture systems have been developed recently. 3D cell culture systems are believed to provide results closer to those that would be obtained *in vivo*. Therefore, this project aimed to develop a 3D model of ameloblast cells by growing HAT-7 cells in Matrigel matrix. Histological structure and gene expression of characteristic ameloblast markers, tight junction proteins and electrolyte transporters in the 3D model were investigated. In addition, the functional activity of HCO_3^- transporters was measured by microfluorometry, and the toxicity of fluoride was tested.

A successful 3D model was developed by culturing HAT-7 cells in Matrigel matrix fed with Hepato-STIM medium. The HAT-7 cells proliferated, differentiated and formed multicellular spheroids. Histology showed that large spheroids presented a lumen, and molecular studies showed that they express the maturation-stage ameloblast marker KLK4, tight-junction proteins cldn-1, cldn-4, cldn-8, TJP1/ZO-1, and electrolyte transporters that play a role in pH regulation and HCO_3^- secretion, namely NHE1, AE1, NBCe1, pendrin and CFTR. Moreover, the spheroids showed similar activities of pH regulatory transporters by microfluorometry as HAT-7 cells grown on permeable supports . In the fluoride toxicity test, 3 mM fluoride destroyed the cells and spheroids while 1mM fluoride affected the formation of the spheres and impaired the cell-cell adhesion structures. In summary, this 3D model is a promising tool for more physiological functional studies of amelogenesis and can also serve as a disease model for certain conditions such as fluorosis. Moreover, this model takes us one step closer to the possibility of *in vivo* tissue repair and tooth regeneration.

7. References

1. Balic A. (2018) Biology Explaining Tooth Repair and Regeneration: A Mini-Review. Gerontology, 64(4):382-388.

2. Nanci A. Structure of the Oral Tissues. Ten Cate's Oral Histology: development, structure, and function. Elsevier, St. Louis (MO), 2018: 1-10.

3. Nanci A. Development of the Tooth and Its Supporting Tissues. Ten Cate's Oral Histology: development, structure, and function. Elsevier, St. Louis (MO), 2018: 68-80.

4. BioRender Templates: BioRender.com. Retrieved June 20, 2021, Available from: https://app.biorender.com/biorender-templates.

5. Zhang W, Yelick PC. (2021) Tooth Repair and Regeneration: Potential of Dental Stem Cells. Trends in Molecular Medicine, 27(5):501-511.

6. Sevari SP, Ansari S, Moshaverinia A. (2021) A narrative overview of utilizing biomaterials to recapitulate the salient regenerative features of dental-derived mesenchymal stem cells. Int J Oral Sci, 13(1):22.

7. Mazzoleni G, Di Lorenzo D, Steimberg N. (2008) Modelling tissues in 3D: the next future of pharmaco-toxicology and food research? Genes & Nutrition, 4(1):13.

8. Breslin S, O'Driscoll L. (2013) Three-dimensional cell culture: the missing link in drug discovery. Drug Discovery Today, 18(5):240-249.

9. Cavalheiro JP, Souza M, Duque CCO, Bussaneli DG, Zuanon Â CC, Jeremias F. (2020) Esthetic rehabilitation of anterior teeth with molar-incisor hypomineralization and dental fluorosis: a case report. Gen Dent, 68(3):34-39.

10. Adserias-Garriga J, Visnapuu V. Age Estimation. Adserias-Garriga J, editor: Academic Press; 2019: 161-168.

11. Kwon H-J, Jiang R. Development of Teeth. Reference Module in Biomedical Sciences, Elsevier, 2018: 1-10.

12. Baranova J, Büchner D, Götz W, Schulze M, Tobiasch E. (2020) Tooth Formation: Are the Hardest Tissues of Human Body Hard to Regenerate? Int J Mol Sci. 21(11):4031.

13. Miletich I, Sharpe PT. (2003) Normal and abnormal dental development. Human Molecular Genetics, 12:69-73.

14. Tompkins K. Molecular mechanisms of cytodifferentiation in mammalian tooth development. (2006) Connect Tissue Res, 47(3):111-118.

15. Thesleff I, Mikkola M. (2002) The role of growth factors in tooth development. Int Rev Cytol, 217:93-135.

16. Miletich I, Sharpe PT. (2004) Neural crest contribution to mammalian tooth formation. Birth Defects Research Part C: Embryo Today: Reviews, 72(2):200-212.

17. Lacruz RS, Habelitz S, Wright JT, Paine ML. (2017) DENTAL ENAMEL FORMATION AND IMPLICATIONS FOR ORAL HEALTH AND DISEASE. Physiol Rev, 97(3):939-993.

18. Thesleff I, Tummers M. Tooth organogenesis and regeneration. Stem book. Cambridge (MA), Harvard Stem Cell Institute; 2008-, 2009: 1-12.

19. Cate ART. (1996) The role of epithelium in the development, structure and function of the tissues of tooth support. Oral Diseases, 2(1):55-62.

20. Huang D, Ren J, Li R, Guan C, Feng Z, Bao B, Wang W, Zhou C. (2020) Tooth Regeneration: Insights from Tooth Development and Spatial-Temporal Control of Bioactive Drug Release. Stem Cell Rev Rep, 16(1):41-55.

21. Lacruz RS. (2017) Enamel: Molecular identity of its transepithelial ion transport system. Cell Calcium, 65:1-7.

22. Cui F-Z, Ge J. (2007) New observations of the hierarchical structure of human enamel, from nanoscale to microscale. Journal of Tissue Engineering and Regenerative Medicine, 1(3):185-191.

23. Smith CEL, Poulter JA, Antanaviciute A, Kirkham J, Brookes SJ, Inglehearn CF, Mighell AJ. (2017) Amelogenesis Imperfecta; Genes, Proteins, and Pathways. Frontiers in Physiology, 8(435):1-22.

24. Varga G, Kerémi B, Bori E, Földes A. (2015) Function and repair of dental enamel – Potential role of epithelial transport processes of ameloblasts. Pancreatology, 15(4, Supplement):S55-S60.

25. Robinson C. (2014) Enamel maturation: a brief background with implications for some enamel dysplasias. Frontiers in Physiology, 5(388):1-6.

26. Aoba T, Fejerskov O. (2002) Dental fluorosis: chemistry and biology. Crit Rev Oral Biol Med, 13(2):155-170.

27. Hu JCC, Chun YHP, Al Hazzazzi T, Simmer JP. (2007) Enamel Formation and Amelogenesis Imperfecta. Cells Tissues Organs, 186(1):78-85.

28. Pindborg JJ, Weinmann JP. (1959) Morphologic and functional correlations in the enamel organ of the rat incisor during amelogenesis. Acta Anat (Basel), 36(4):367-81.
29. Robinson C, Kirkham J, Briggs HD, Atkinson PJ. (1982) Enamel proteins: from secretion to maturation. J Dent Res, Spec No:1490-1495.
30. Fincham AG, Moradian-Oldak J, Simmer JP. (1999) The structural biology of the developing dental enamel matrix. J Struct Biol, 126(3):270-299.
31. Wang L, Guan X, Du C, Moradian-Oldak J, Nancollas GH. (2007) Amelogenin Promotes the Formation of Elongated Apatite Microstructures in a Controlled Crystallization System. J Phys Chem C Nanomater Interfaces, 111(17):6398-6404.
32. Aoba T, Tanabe T, Moreno EC. (1987) Function of amelogenins in porcine enamel mineralization during the secretory stage of amelogenesis. Adv Dent Res, 1(2):252-260.
33. Krebsbach PH, Lee SK, Matsuki Y, Kozak CA, Yamada KM, Yamada Y. (1996) Full-length Sequence, Localization, and Chromosomal Mapping of Ameloblastin: A NOVEL TOOTH-SPECIFIC GENE. Journal of Biological Chemistry, 271(8):4431-4435.
34. Fukumoto S, Kiba T, Hall B, Iehara N, Nakamura T, Longenecker G, Krebsbach PH H, Nanci A, Kulkarni AB, Yamada Y. (2004) Ameloblastin is a cell adhesion molecule required for maintaining the differentiation state of ameloblasts. J Cell Biol, 167(5):973-983.
35. Hu CC, Fukae M, Uchida T, Qian Q, Zhang CH, Ryu OH, Tanabe T, Yamakoshi Y, Murakami C, Dohi N, Shimizu M, Simmer JP. (1997) Cloning and characterization of porcine enamelin mRNAs. J Dent Res, 76(11):1720-1729.
36. Hu CC, Hart TC, Dupont BR, Chen JJ, Sun X, Qian Q, Zhang CH, Jiang H, Mattern V L, Wright J T, Simmer J P. (2000) Cloning human enamelin cDNA, chromosomal localization, and analysis of expression during tooth development. J Dent Res, 79(4):912-919.
37. Hu JC, Hu Y, Lu Y, Smith CE, Lertlam R, Wright JT, Suggs C, McKee MD, Beniash E, Kabir ME, Simmer JP. (2014) Enamelin is critical for ameloblast integrity and enamel ultrastructure formation. PLoS One, 9(3):e89303.
38. Lacruz RS, Smith CE, Chen YB, Hubbard MJ, Hacia JG, Paine ML. (2011) Gene-expression analysis of early- and late-maturation-stage rat enamel organ. Eur J Oral Sci, 119:149-157.

39. Mårdh CK, Bäckman B, Holmgren Gs, Hu JC-C, Simmer JP, Forsman-Semb K. (2002) A nonsense mutation in the enamelin gene causes local hypoplastic autosomal dominant amelogenesis imperfecta (AIH2). Human Molecular Genetics, 11(9):1069-1074.

40. Liang T, Hu Y, Smith CE, Richardson AS, Zhang H, Yang J, Lin B, Wang SK, Kim JW, Chun YH, Simmer JP, Hu JC. (2019) AMBN mutations causing hypoplastic amelogenesis imperfecta and Ambn knockout-NLS-lacZ knockin mice exhibiting failed amelogenesis and Ambn tissue-specificity. Mol Genet Genomic Med, 7(9):e929.

41. Hu JC, Chan HC, Simmer SG, Seymen F, Richardson AS, Hu Y, Milkovich RN, Estrella NM, Yildirim M, Bayram M, Chen CF, Simmer JP. (2012) Amelogenesis imperfecta in two families with defined AMELX deletions in ARHGAP6. PLoS One, 7(12):e52052.

42. Gibson CW, Yuan ZA, Hall B, Longenecker G, Chen E, Thyagarajan T, Sreenath T, Wright JT, Decker S, Piddington R, Harrison G, Kulkarni AB. (2001) Amelogenin-deficient mice display an amelogenesis imperfecta phenotype. J Biol Chem, 276(34):31871-31875.

43. Llano E, Pendás AM, Knäuper V, Sorsa T, Salo T, Salido E, Murphy G, Simmer JP, Bartlett JD, López-Otín C. (1997) Identification and structural and functional characterization of human enamelysin (MMP-20). Biochemistry, 36(49):15101-15108.

44. Ryu OH, Fincham AG, Hu CC, Zhang C, Qian Q, Bartlett JD, Simmer, JP. (1999) Characterization of recombinant pig enamelysin activity and cleavage of recombinant pig and mouse amelogenins. J Dent Res, 78(3):743-750.

45. Caterina JJ, Skobe Z, Shi J, Ding Y, Simmer JP, Birkedal-Hansen H, Bartlett JD. (2002) Enamelysin (matrix metalloproteinase 20)-deficient mice display an amelogenesis imperfecta phenotype. J Biol Chem. 277(51):49598-49604.

46. Yin K, Hacia JG, Zhong Z, Paine ML. (2014) Genome-wide analysis of miRNA and mRNA transcriptomes during amelogenesis. BMC Genomics, 15(1):998.

47. Simmer JP, Richardson AS, Wang SK, Reid BM, Bai Y, Hu Y, Hu, JC. (2014) Ameloblast transcriptome changes from secretory to maturation stages. Connect Tissue Res, 55(1):29-32.

48. Lacruz RS, Smith CE, Bringas Jr P, Chen Y-B, Smith SM, Snead ML, Kurtz IH. Joseph G, Hubbard MJ, Paine ML. (2012) Identification of novel candidate genes involved in mineralization of dental enamel by genome-wide transcript profiling. Journal of Cellular Physiology, 227(5):2264-2275.

49. Josephsen K, Fejerskov O. (1997) Ameloblast modulation in the maturation zone of the rat incisor enamel organ. A light and electron microscopic study. J Anat, 124(1):45-70.

50. Simmer JP, Fincham AG. (1995) Molecular mechanisms of dental enamel formation. Crit Rev Oral Biol Med, 6(2):84-108.

51. Skobe Z, Prostak KS, Stern DN. (1988) A scanning electron microscope study of monkey maturation-stage ameloblasts. J Dent Res, 67(11):1396-1401.

52. Moffatt P, Smith CE, St-Arnaud R, Simmons D, Wright JT, Nanci A. (2006) Cloning of rat amelotin and localization of the protein to the basal lamina of maturation stage ameloblasts and junctional epithelium. Biochem J, 399(1):37-46.

53. Iwasaki K, Bajenova E, Somogyi-Ganss E, Miller M, Nguyen V, Nourkeyhani H, Nourkeyhani, H, Gao Y, Wendel M, Ganss B. (2005) Amelotin--a Novel Secreted, Ameloblast-specific Protein. J Dent Res, 84(12):1127-1132.

54. Moffatt P, Wazen RM, Dos Santos Neves J, Nanci A. (2014) Characterisation of secretory calcium-binding phosphoprotein-proline-glutamine-rich 1: a novel basal lamina component expressed at cell-tooth interfaces. Cell Tissue Res, 358(3):843-855.

55. Moffatt P, Smith CE, St-Arnaud R, Nanci A. (2008) Characterization of Apin, a secreted protein highly expressed in tooth-associated epithelia. J Cell Biochem. 103(3):941-956.

56. Park JC, Park JT, Son HH, Kim HJ, Jeong MJ, Lee CS, Dey R, Cho MI. (2007) The amyloid protein APin is highly expressed during enamel mineralization and maturation in rat incisors. Eur J Oral Sci, 115(2):153-160.

57. Dos Santos Neves J, Wazen RM, Kuroda S, Francis Zalzal S, Moffatt P, Nanci A. (2012) Odontogenic ameloblast-associated and amelotin are novel basal lamina components. Histochem Cell Biol, 137(3):329-338.

58. Abbarin N, San Miguel S, Holcroft J, Iwasaki K, Ganss B. (2015) The enamel protein amelotin is a promoter of hydroxyapatite mineralization. J Bone Miner Res, 30(5):775-785.

59. Nakayama Y, Holcroft J, Ganss B. (2015) Enamel Hypomineralization and Structural Defects in Amelotin-deficient Mice. J Dent Res, 94(5):697-705.
60. Huysmans MC, Young A, Ganss C. (2014) The role of fluoride in erosion therapy. Monogr Oral Sci, 25:230-243.
61. Hu Y, Hu JC, Smith CE, Bartlett JD, Simmer JP. (2011) Kallikrein-related peptidase 4, matrix metalloproteinase 20, and the maturation of murine and porcine enamel. Eur J Oral Sci, 119 (1):217-225.
62. Smith CE. (1998) Cellular and chemical events during enamel maturation. Crit Rev Oral Biol Med, 9(2):128-161.
63. Robinson C, Kirkham J, Brookes SJ, Bonass WA, Shore RC. (1995) The chemistry of enamel development. Int J Dev Biol, 39(1):145-152.
64. Lacruz RS, Nanci A, Kurtz I, Wright JT, Paine ML. (2010) Regulation of pH During Amelogenesis. Calcified Tissue International, 86(2):91-103.
65. Varga G, DenBesten P, Rácz R, Zsembery Á. (2018) Importance of bicarbonate transport in pH control during amelogenesis — need for functional studies. Oral Diseases, 24(6):879-890.
66. Bori E, Guo J, Rácz R, Burghardt B, Földes A, Kerémi B, Harada H, Steward MC, Den Besten P, Bronckers AL, Varga G. (2016) Evidence for Bicarbonate Secretion by Ameloblasts in a Novel Cellular Model. J Dent Res, 95(5):588-596.
67. Rácz R, Földes A, Bori E, Zsembery Á, Harada H, Steward MC, DenBesten P, Bronckers AL, Gerber G, Varga G. (2017) No Change in Bicarbonate Transport but Tight-Junction Formation Is Delayed by Fluoride in a Novel Ameloblast Model. Front Physiol, 8:940.
68. Sasaki S, Takagi T, Suzuki M. (1991) Cyclical changes in pH in bovine developing enamel as sequential bands. Arch Oral Biol, 36(3):227-231.
69. Lyman GE, Waddell WJ. (1977) pH gradients in the developing teeth of young mice from autoradiography of [14C]DMO. Am J Physiol, 232(4):364-367.
70. Smith CE, Issid M, Margolis HC, Moreno EC. (1996) Developmental changes in the pH of enamel fluid and its effects on matrix-resident proteinases. Adv Dent Res, 10(2):159-169.
71. Ji M, Xiao L, Xu L, Huang S, Zhang D. (2018) How pH is regulated during amelogenesis in dental fluorosis. Exp Ther Med, 16(5):3759-3765.

72. Kakei M, Nakahara H. (1996) Aspects of carbonic anhydrase and carbonate content during mineralization of the rat enamel. Biochim Biophys Acta, 1289(2):226-230.
73. Lin HM, Nakamura H, Noda T, Ozawa H. (1994) Localization of H(+)-ATPase and carbonic anhydrase II in ameloblasts at maturation. Calcif Tissue Int, 55(1):38-45.
74. Smith CE, Nanci A, Moffatt P. (2006) Evidence by signal peptide trap technology for the expression of carbonic anhydrase 6 in rat incisor enamel organs. Eur J Oral Sci, 114:147-153.
75. Toyosawa S, Ogawa Y, Inagaki T, Ijuhin N. (1996) Immunohistochemical localization of carbonic anhydrase isozyme II in rat incisor epithelial cells at various stages of amelogenesis. Cell Tissue Res, 285(2):217-225.
76. Racz R, Nagy A, Rakonczay Z, Dunavari EK, Gerber G, Varga G. (2018) Defense Mechanisms Against Acid Exposure by Dental Enamel Formation, Saliva and Pancreatic Juice Production. Curr Pharm Des, 24(18):2012-2022.
77. Supuran CT. (2008) Carbonic anhydrases--an overview. Curr Pharm Des, 14(7):603-614.
78. Sly WS, Hu PY. (1995) HUMAN CARBONIC ANHYDRASES AND CARBONIC ANHYDRASE DEFICIENCIES. Annual Review of Biochemistry, 64(1):375-401.
79. Dogterom AA, Bronckers AL. (1983) Carbonic anhydrase in developing hamster molars. J Dent Res, 62(7):789-791.
80. Josephsen K, Takano Y, Frische S, Praetorius J, Nielsen S, Aoba T, Fejerskov O. (2010) Ion transporters in secretory and cyclically modulating ameloblasts: a new hypothesis for cellular control of preeruptive enamel maturation. Am J Physiol Cell Physiol, 299(6):1299-12307.
81. Hediger MA, Romero MF, Peng J-B, Rolfs A, Takanaga H, Bruford EA. (2004) The ABCs of solute carriers: physiological, pathological and therapeutic implications of human membrane transport proteins. Pflügers Archiv, 447(5):465-468.
82. Lyaruu DM, Bronckers AL, Mulder L, Mardones P, Medina JF, Kellokumpu S, Oude Elferink RP, Everts V. (2008) The anion exchanger Ae2 is required for enamel maturation in mouse teeth. Matrix Biol, 27(2):119-127.
83. Paine ML, Snead ML, Wang HJ, Abuladze N, Pushkin A, Liu W, Kao LY, Wall SM, Kim YH, Kurtz I. (2008) Role of NBCe1 and AE2 in secretory ameloblasts. J Dent Res, 87(4):391-395.

84. Bronckers AL. (2017) Ion Transport by Ameloblasts during Amelogenesis. J Dent Res, 96(3):243-253.

85. Lacruz RS, Nanci A, White SN, Wen X, Wang H, Zalzal SF, Luong VQ, Schuetter VL, Conti PS, Kurtz I, Paine ML. (2010) The sodium bicarbonate cotransporter (NBCe1) is essential for normal development of mouse dentition. J Biol Chem, 285(32):24432-24438.

86. Bronckers ALJJ, Guo J, Zandieh-Doulabi B, Bervoets TJ, Lyaruu DM, Li X, Wangemann P. DenBesten P. (2011) Developmental expression of solute carrier family 26A member 4 (SLC26A4/pendrin) during amelogenesis in developing rodent teeth. European Journal of Oral Sciences, 119(s1):185-192.

87. Jalali R, Zandieh-Doulabi B, DenBesten PK, Seidler U, Riederer B, Wedenoja S, Micha D, Bronckers AL. (2015) Slc26a3/Dra and Slc26a6 in Murine Ameloblasts. J Dent Res, 94(12):1732-1739.

88. Seidler U, Nikolovska K. (2019) Slc26 Family of Anion Transporters in the Gastrointestinal Tract: Expression, Function, Regulation, and Role in Disease. Compr Physiol, 9(2):839-872.

89. Bronckers A, Kalogeraki L, Jorna HJ, Wilke M, Bervoets TJ, Lyaruu DM, Zandieh-Doulabi B, Denbesten P, de Jonge H. (2010) The cystic fibrosis transmembrane conductance regulator (CFTR) is expressed in maturation stage ameloblasts, odontoblasts and bone cells. Bone, 46(4):1188-1196.

90. Wang XF, Zhou CX, Shi QX, Yuan YY, Yu MK, Ajonuma LC, Ho LS, Lo PS, Tsang LL, Liu Y, Lam SY, Chan LN, Zhao WC, Chung YW, Chan HC. (2003) Involvement of CFTR in uterine bicarbonate secretion and the fertilizing capacity of sperm. Nat Cell Biol, 5(10):902-906.

91. Crawford I, Maloney PC, Zeitlin PL, Guggino WB, Hyde SC, Turley H, Gatter KC, Harris A, Higgins CF. (1991) Immunocytochemical localization of the cystic fibrosis gene product CFTR. Proc Natl Acad Sci U S A, 88(20):9262-9266.

92. Ishiguro H, Steward MC, Naruse S, Ko SB, Goto H, Case RM, Kondo T, Yamamoto A. (2009) CFTR functions as a bicarbonate channel in pancreatic duct cells. J Gen Physiol, 133(3):315-326.

93. Lee MG, Choi JY, Luo X, Strickland E, Thomas PJ, Muallem S. (1999) Cystic Fibrosis Transmembrane Conductance Regulator Regulates Luminal

$Cl^-/HCO3^-$Exchange in Mouse Submandibular and Pancreatic Ducts. Journal of Biological Chemistry, 274(21):14670-14677.

94. Arquitt CK, Boyd C, Wright JT. (2002) Cystic fibrosis transmembrane regulator gene (CFTR) is associated with abnormal enamel formation. J Dent Res, 81(7):492-496.

95. Sui W, Boyd C, Wright JT. (2003) Altered pH regulation during enamel development in the cystic fibrosis mouse incisor. J Dent Res, 82(5):388-392.

96. Wright JT, Kiefer CL, Hall KI, Grubb BR. (1996) Abnormal enamel development in a cystic fibrosis transgenic mouse model. J Dent Res, 75(4):966-973.

97. Wright JT, Hall KI, Grubb BR. (19960 Enamel mineral composition of normal and cystic fibrosis transgenic mice. Adv Dent Res, 10(2):270-274.

98. Chang EH, Lacruz RS, Bromage TG, Bringas P, Jr., Welsh MJ, Zabner J, Paine, ML. (2011) Enamel pathology resulting from loss of function in the cystic fibrosis transmembrane conductance regulator in a porcine animal model. Cells Tissues Organs, 194(2-4):249-254.

99. Collins FS. (1992) Cystic fibrosis: molecular biology and therapeutic implications. Science, 256(5058):774-779.

100. Azevedo TD, Feijó GC, Bezerra AC. (2006) Presence of developmental defects of enamel in cystic fibrosis patients. J Dent Child (Chic), 73(3):159-163.

101. Cua FT. (1991) Calcium and phosphorous in teeth from children with and without cystic fibrosis. Biol Trace Elem Res, 30(3):277-289.

102. Ferrazzano GF, Sangianantoni G, Cantile T, Amato I, Orlando S, Ingenito A. (2012) Dental enamel defects in Italian children with cystic fibrosis: an observational study. Community Dent Health, 29(1):106-109.

103. Zegarelli EV, Kutscher AH, Denning CR, Applebaum E, Fahn BS, Hoffman PJ, Botwick JT, Ragosta JM. (1964) DISCOLORATION OF THE TEETH IN OLDER CHILDREN WITH CYSTIC FIBROSIS OF THE PANCREAS. Am J Dig Dis, 9:682-683.

104. DenBesten P, Li W. (2011) Chronic fluoride toxicity: dental fluorosis. Monogr Oral Sci, 22:81-96.

105. Bronckers AL, Lyaruu DM, DenBesten PK. (2009) The impact of fluoride on ameloblasts and the mechanisms of enamel fluorosis. J Dent Res, 88(10):877-893.

106. Zou J, Ashley JW. Fluorosis. Pathobiology of Human Disease. Academic Press, San Diego, 2014: 893-898.

107. Zhang Y, Zhang K, Ma L, Gu H, Li J, Lei S. (2016) Fluoride induced endoplasmic reticulum stress and calcium overload in ameloblasts. Arch Oral Biol, 69:95-101.

108. Angwa LM, Jiang Y, Pei J, Sun D. Antioxidant Phytochemicals for the Prevention of Fluoride-Induced Oxidative Stress and Apoptosis: a Review. Biol Trace Elem Res. 2021:1418-1441.

109. Barbier O, Arreola-Mendoza L, Del Razo LM. (2010) Molecular mechanisms of fluoride toxicity. Chemico-Biological Interactions, 188(2):319-333.

110. Fujiwara N, Whitford GM, Bartlett JD, Suzuki M. (2021) Curcumin suppresses cell growth and attenuates fluoride-mediated Caspase-3 activation in ameloblast-like LS8 cells. Environ Pollut, 273:116495.

111. Sharma R, Tsuchiya M, Bartlett JD. (2008) Fluoride induces endoplasmic reticulum stress and inhibits protein synthesis and secretion. Environ Health Perspect, 116(9):1142-1146.

112. Wang Y, Li A, Mehmood K, Hussain R, Abbas RZ, Javed MT, Chang YF, Hu L, Pan J, Li Y, Shi L, Tang Z, Zhang H. (2021) Long-term exposure to the fluoride blocks the development of chondrocytes in the ducks: The molecular mechanism of fluoride regulating autophagy and apoptosis. Ecotoxicol Environ Saf, 217:112225.

113. Zhao L, Li J, Su J, Snead ML, Ruan J. (2016) LS8 cell apoptosis induced by NaF through p-ERK and p-JNK - a mechanism study of dental fluorosis. Acta Odontol Scand, 74(7):539-549.

114. Dean HT. (1956) Fluorine in the control of dental caries. The Journal of the American Dental Association, 52(1):1-8.

115. Di Giovanni T, Eliades T, Papageorgiou SN. (2018) Interventions for dental fluorosis: A systematic review. J Esthet Restor Dent, 30(6):502-508.

116. Skardal A. Essentials of 3D Biofabrication and Translation. Academic Press, Boston, 2015: 1-17.

117. Lanza R, Atala A. 'Stemness':Definitions, Criteria, and Standards. Essentials of Stem Cell Biology. Academic Press, Boston, 2013: 7-17.

118. Silva Couto P, Rotondi MC, Bersenev A, Hewitt CJ, Nienow AW, Verter F, Rafiq QA. (2020) Expansion of human mesenchymal stem/stromal cells (hMSCs) in bioreactors

using microcarriers: lessons learnt and what the future holds. Biotechnology Advances, 45:107636.

119. Peng L, Ye L, Zhou XD. (2009) Mesenchymal stem cells and tooth engineering. Int J Oral Sci. 1(1):6-12.

120. Zhou H, Wu S, Joo JY, Zhu S, Han DW, Lin T, Trauger S, Bien G, Yao S, Zhu Y, Siuzdak G, Schöler HR, Duan L, Ding S. (2009) Generation of induced pluripotent stem cells using recombinant proteins. Cell Stem Cell. 4(5):381-384.

121. Prokhorova TA, Harkness LM, Frandsen U, Ditzel N, Schrøder HD, Burns JS, Kassem, M. (2009) Teratoma formation by human embryonic stem cells is site dependent and enhanced by the presence of Matrigel. Stem Cells Dev. 18(1):47-54.

122. Galmiche MC, Koteliansky VE, Briere J, Herve P, Charbord P. (1993) Stromal cells from human long-term marrow cultures are mesenchymal cells that differentiate following a vascular smooth muscle differentiation pathway. Blood, 82(1):66-76.

123. Muguruma Y, Yahata T, Miyatake H, Sato T, Uno T, Itoh J, Kato S, Ito M, Hotta T, Ando K. (2006) Reconstitution of the functional human hematopoietic microenvironment derived from human mesenchymal stem cells in the murine bone marrow compartment. Blood, 107(5):1878-1887.

124. Petersen BE, Bowen WC, Patrene KD, Mars WM, Sullivan AK, Murase N, Boggs SS, Greenberger JS, Goff JP. (1999) Bone marrow as a potential source of hepatic oval cells. Science, 284(5417):1168-1170.

125. Gerecht-Nir S, Itskovitz-Eldor J. (2004) Human embryonic stem cells: A potential source for cellular therapy. American Journal of Transplantation, 4(s6):51-57.

126. Wang W, Itaka K, Ohba S, Nishiyama N, Chung U-i, Yamasaki Y, Kataoka K. (2009) 3D spheroid culture system on micropatterned substrates for improved differentiation efficiency of multipotent mesenchymal stem cells. Biomaterials, 30(14):2705-2715.

127. Abuarqoub D, Aslam N, Almajali B, Shajrawi L, Jafar H, Awidi A. (2020) Neuro-regenerative potential of dental stem cells: a concise review. Cell Tissue Res, 382(2):267-279.

128. Zhai Q, Dong Z, Wang W, Li B, Jin Y. (2019) Dental stem cell and dental tissue regeneration. Frontiers of Medicine, 13(2):152-159.

129. Gronthos S, Mankani M, Brahim J, Robey PG, Shi S. (2000) Postnatal human dental pulp stem cells (DPSCs) in vitro and in vivo. Proceedings of the National Academy of Sciences, 97(25):13625.

130. Varga G, Gerber G. (2014) Mesenchymal stem cells of dental origin as promising tools for neuroregeneration. Stem Cell Res Ther, 5(2):61.

131. Khaseb S, Orooji M, Pour MG, Safavi SM, Eghbal MJ, Rezai Rad M. Dental stem cell banking: Techniques and protocols. Cell Biol Int. 2021:1851-1865.

132. Miura M, Gronthos S, Zhao M, Lu B, Fisher LW, Robey PG, Shi S. (2003) SHED: Stem cells from human exfoliated deciduous teeth. Proceedings of the National Academy of Sciences, 100(10):5807.

133. Seo B-M, Miura M, Gronthos S, Mark Bartold P, Batouli S, Brahim J, Young M, Gehron Robey P, Wang CY, Shi S. (2004) Investigation of multipotent postnatal stem cells from human periodontal ligament. The Lancet, 364(9429):149-155.

134. Morsczeck C, Moehl C, Götz W, Heredia A, Schäffer TE, Eckstein N, Sippel C, Hoffmann KH. (2005) In vitro differentiation of human dental follicle cells with dexamethasone and insulin. Cell Biol Int, 29(7):567-575.

135. Sonoyama W, Liu Y, Fang D, Yamaza T, Seo BM, Zhang C, Liu H, Gronthos S, Wang CY, Wang S, Shi S. (2006) Mesenchymal stem cell-mediated functional tooth regeneration in swine. PLoS One, 1(1):e79.

136. Huang GT-J, Gronthos S, Shi S. (2009) Mesenchymal Stem Cells Derived from Dental Tissues vs. Those from Other Sources: Their Biology and Role in Regenerative Medicine. Journal of Dental Research, 88(9):792-806.

137. Liu J, Yu F, Sun Y, Jiang B, Zhang W, Yang J, Xu GT, Liang A, Liu S. (2015) Concise reviews: Characteristics and potential applications of human dental tissue-derived mesenchymal stem cells. Stem Cells, 33(3):627-638.

138. Nuti N, Corallo C, Chan BMF, Ferrari M, Gerami-Naini B. (2016) Multipotent Differentiation of Human Dental Pulp Stem Cells: a Literature Review. Stem Cell Reviews and Reports, 12(5):511-523.

139. Villarroel V, Fagalde P, Reininger D. (2021) Potential therapeutic uses of intraoral mesenchymal stem cells in other tissues of the body: A review. J Clin Exp Dent, 13(3):e259-e67.

140. Morsczeck C, Reichert TE. (2018) Dental stem cells in tooth regeneration and repair in the future. Expert Opinion on Biological Therapy, 18(2):187-196.

141. Rodríguez-Hernandez C, Torres-García S, Olvera C, Ramírez Castillo F, Loera Muro A, González F, Guerrero-Barrera A. (2014) Cell culture: History, Development and Prospects. International Journal of Current Research and Academic Review, 2:188-200.

142. Segeritz CP, Vallier L. (2017) Cell Culture: Growing Cells as Model Systems In Vitro. Basic Science Methods for Clinical Researchers, 151-172.

143. Kapałczyńska M, Kolenda T, Przybyła W, Zajączkowska M, Teresiak A, Filas V, Ibbs M, Bliźniak R, Łuczewski Ł, Lamperska K. (2018) 2D and 3D cell cultures - a comparison of different types of cancer cell cultures. Arch Med Sci, 14(4):910-919.

144. Goodman SR. Tools of the Cell Biologist, Goodman's Medical Cell Biology. Academic Press, 2021: 1-24.

145. Chaicharoenaudomrung N, Kunhorm P, Noisa P. (2019) Three-dimensional cell culture systems as an in vitro platform for cancer and stem cell modeling. World J Stem Cells, 11(12):1065-1083.

146. Edmondson R, Broglie JJ, Adcock AF, Yang L. (2014) Three-Dimensional Cell Culture Systems and Their Applications in Drug Discovery and Cell-Based Biosensors. ASSAY and Drug Development Technologies, 12(4):207-218.

147. Fang Y, Eglen RM. (2017) Three-Dimensional Cell Cultures in Drug Discovery and Development. SLAS DISCOVERY: Advancing the Science of Drug Discovery, 22(5):456-472.

148. Pampaloni F, Reynaud EG, Stelzer EHK. (2007) The third dimension bridges the gap between cell culture and live tissue. Nature Reviews Molecular Cell Biology, 8(10):839-845.

149. Kleinman HK, Martin GR. (2005) Matrigel: basement membrane matrix with biological activity. Semin Cancer Biol, 15(5):378-386.

150. Lee GY, Kenny PA, Lee EH, Bissell MJ. (2007) Three-dimensional culture models of normal and malignant breast epithelial cells. Nat Methods, 4(4):359-365.

151. Szlávik V, Szabó B, Vicsek T, Barabás J, Bogdán S, Gresz V, Varga G, O'Connell B, Vág J. (2008) Differentiation of primary human submandibular gland cells cultured on basement membrane extract. Tissue Eng Part A, 14(11):1915-1926.

152. Hoffman MP, Kibbey MC, Letterio JJ, Kleinman HK. (1996) Role of laminin-1 and TGF-beta 3 in acinar differentiation of a human submandibular gland cell line (HSG). J Cell Sci, 109(8):2013-2021.

153. Kubota Y, Kleinman HK, Martin GR, Lawley TJ. (1988) Role of laminin and basement membrane in the morphological differentiation of human endothelial cells into capillary-like structures. Journal of Cell Biology, 107(4):1589-1598.

154. Kawano S, Morotomi T, Toyono T, Nakamura N, Uchida T, Ohishi M, Toyoshima K, Harada H. (2002) Establishment of Dental Epithelial Cell Line (HAT-7) and the Cell Differentiation Dependent on Notch Signaling Pathway. Connective Tissue Research, 43(2-3):409-412.

155. Jalali R, Lodder JC, Zandieh-Doulabi B, Micha D, Melvin JE, Catalan MA, Mansvelder HD, DenBesten P, Bronckers A. (2017) The Role of Na:K:2Cl Cotransporter 1 (NKCC1/SLC12A2) in Dental Epithelium during Enamel Formation in Mice. Front Physiol, 8:924.

156. Mahdee AF, Ali AH, Gillespie JI. (2021) Structural and functional relations between the connective tissue and epithelium of enamel organ and their role during enamel maturation. Journal of Molecular Histology, 52(5):975-989.

157. de Isla N, Huseltein C, Jessel N, Pinzano A, Decot V, Magdalou J, Bensoussan D, Stoltz JF. (2010) Introduction to tissue engineering and application for cartilage engineering. Biomed Mater Eng, 20(3):127-133.

158. Zhu Y, Zhang P, Gu RL, Liu YS, Zhou YS. (2018) Origin and Clinical Applications of Neural Crest-Derived Dental Stem Cells. Chin J Dent Res, 21(2):89-100.

159. Hegyesi O, Földes A, Bori E, Németh Z, Barabás J, Steward MC, Varga, G. (2015) Evidence for Active Electrolyte Transport by Two-Dimensional Monolayers of Human Salivary Epithelial Cells. Tissue Eng Part C Methods. 21(12):1226-1236.

160. Maria OM, Zeitouni A, Gologan O, Tran SD. (2011) Matrigel improves functional properties of primary human salivary gland cells. Tissue Eng Part A, 17(9-10):1229-1238.

161. Schönthal AH, Warren DW, Stevenson D, Schecter JE, Azzarolo AM, Mircheff AK, Trousdale MD. (2000) Proliferation of Lacrimal Gland Acinar Cells in Primary Culture. Stimulation by Extracellular Matrix, EGF, and DHT. Experimental Eye Research, 70(5):639-649.

162. Tiwari S, Nair RM, Vamadevan P, Ali MJ, Naik MN, Honavar SG, Vemuganti GK. (2018) Establishing and characterizing lacrispheres from human lacrimal gland for potential clinical application. Graefes Arch Clin Exp Ophthalmol, 256(4):717-727.
163. Altay G, Batlle E, Fernández-Majada V, Martinez E. (2020) In vitro Self-organized Mouse Small Intestinal Epithelial Monolayer Protocol. Bio Protoc, 10(3):e3514.
164. Delbue D, Lebenheim L, Cardoso-Silva D, Dony V, Krug SM, Richter JF, Manna S, Muñoz M, Wolk K, Heldt C, Heimesaat MM, Sabat R, Siegmund B, Schumann M. (2021) Reprogramming Intestinal Epithelial Cell Polarity by Interleukin-22. Front Med (Lausanne), 8:656047.
165. Massie I, Spaniol K, Barbian A, Geerling G, Metzger M, Schrader S. (2018) Development of lacrimal gland spheroids for lacrimal gland tissue regeneration. Journal of Tissue Engineering and Regenerative MedicinE, 12(4):e2001-e2009.
166. Huang J, Jiang Y, Ren Y, Liu Y, Wu X, Li Z, Wang W, Zhou C. (2020) Biomaterials and biosensors in intestinal organoid culture, a progress review. J Biomed Mater Res A, 108(7):1501-1508.
167. Bakhti M, Scheibner K, Tritschler S, Bastidas-Ponce A, Tarquis-Medina M, Theis FJ, Lickert H. (2019) Establishment of a high-resolution 3D modeling system for studying pancreatic epithelial cell biology in vitro. Mol Metab, 30:16-29.
168. Molnár R, Madácsy T, Varga Á, Németh M, Katona X, Görög M, Molnár B, Fanczal J, Rakonczay Z, Hegyi P, Pallagi P, Maléth J. (2020) Mouse pancreatic ductal organoid culture as a relevant model to study exocrine pancreatic ion secretion. Laboratory Investigation,100(1):84-97.
169. Szlávik V, Vág J, Markó K, Demeter K, Madarász E, Oláh I, Zelles T, O'Connell BC, Varga G. (2008) Matrigel-induced acinar differentiation is followed by apoptosis in HSG cells. Journal of Cellular Biochemistry, 103(1):284-295.
170. Li W, Machule D, Gao C, DenBesten PK. (2006) Growth of ameloblast-lineage cells in a three-dimensional Matrigel environment. European Journal of Oral Sciences, 114(1):159-163.
171. Natsiou D, Granchi Z, Mitsiadis TA, Jimenez-Rojo L. (2017) Generation of Spheres from Dental Epithelial Stem Cells. Front Physiol, 8:7.
172. Griffith LG, Swartz MA. (2006) Capturing complex 3D tissue physiology in vitro. Nat Rev Mol Cell Biol, 7(3):211-224.

173. Roignot J, Peng X, Mostov K. (2013) Polarity in mammalian epithelial morphogenesis. Cold Spring Harb Perspect Biol, 5(2):a013789.

174. Zegers MMP, O'Brien LE, Yu W, Datta A, Mostov KE. (2003) Epithelial polarity and tubulogenesis in vitro. Trends in Cell Biology, 13(4):169-176.

175. He P, Zhang Y, Kim SO, Radlanski RJ, Butcher K, Schneider RA, DenBesten PK. (2010) Ameloblast differentiation in the human developing tooth: Effects of extracellular matrices. Matrix Biology,29(5):411-419.

176. Zheng L, Warotayanont R, Stahl J, Kunimatsu R, Klein O, DenBesten PK, Zhang Y. (2013) Inductive ability of human developing and differentiated dental mesenchyme. Cells Tissues Organs, 198(2):99-110.

177. Zheng LW, Linthicum L, DenBesten PK, Zhang Y. (2013) The similarity between human embryonic stem cell-derived epithelial cells and ameloblast-lineage cells. Int J Oral Sci, 5(1):1-6.

178. Hata M, Kawamoto T, Kawai M, Yamamoto T. (2010) Differential expression patterns of the tight junction-associated proteins occludin and claudins in secretory and mature ameloblasts in mouse incisor. Med Mol Morphol,43(2):102-106.

179. Inai T, Sengoku A, Hirose E, Iida H, Shibata Y. (2008) Differential expression of the tight junction proteins, claudin-1, claudin-4, occludin, ZO-1, and PAR3, in the ameloblasts of rat upper incisors. Anat Rec (Hoboken), 291(5):577-585.

180. Amasheh S, Milatz S, Krug SM, Bergs M, Amasheh M, Schulzke JD, Fromm M. (2009) Na+ absorption defends from paracellular back-leakage by claudin-8 upregulation. Biochem Biophys Res Commun, 378(1):45-50.

181. Bronckers AL, Lyaruu DM, Guo J, Bijvelds MJ, Bervoets TJ, Zandieh-Doulabi B, Medina JF, Li Z, Zhang Y, DenBesten PK. (2015) Composition of mineralizing incisor enamel in cystic fibrosis transmembrane conductance regulator-deficient mice. Eur J Oral Sci. 123(1):9-16.

182. Suzuki M, Bandoski C, Bartlett JD. (2015) Fluoride induces oxidative damage and SIRT1/autophagy through ROS-mediated JNK signaling. Free Radic Biol Med, 89:369-378.

183. Yan Q, Zhang Y, Li W, Denbesten PK. (2007) Micromolar fluoride alters ameloblast lineage cells in vitro. J Dent Res, 86(4):336-340.

184. Zhang Y, Yan Q, Li W, DenBesten PK. (2006) Fluoride down-regulates the expression of matrix metalloproteinase-20 in human fetal tooth ameloblast-lineage cells in vitro. Eur J Oral Sci, 114(1):105-110.

185. Zhang Y, Li W, Chi HS, Chen J, Denbesten PK. (2007) JNK/c-Jun signaling pathway mediates the fluoride-induced down-regulation of MMP-20 in vitro. Matrix Biol, 26(8):633-641.

The bibliography of the candidate's publications

Publications related to the thesis

1. Földes, A., **Sang-Ngoen, T.**, Kádár, K., Rácz, R., Zsembery, Á., DenBesten, P., Steward, M. C., & Varga, G. (2021). Three-Dimensional Culture of Ameloblast-Originated HAT-7 Cells for Functional Modeling of Defective Tooth Enamel Formation. **Frontiers in pharmacology**, 12, 682654. https://doi.org/10.3389/fphar.2021.682654
IF: 5.811

2. Perczel-Kovách, K., Hegedűs, O., Földes, A., **Sangngoen, T.**, Kálló, K., Steward, M. C., Varga, G., & Nagy, K. S. (2021). STRO-1 positive cell expansion during osteogenic differentiation: A comparative study of three mesenchymal stem cell types of dental origin. **Archives of oral biology**, 122, 104995. https://doi.org/10.1016/j.archoralbio.2020.104995
IF: 2.635

Publications unrelated to the thesis

1. **Sang-ngoen T.**, Czumbel L. M., Sadaeng W., Mikó A., Német I. D., Mátrai P., Hegyi P., Tóth B., Csupor D., Kiss I., Szabó A., Gerber G., Varga G., Kerémi B. (2021). Orally administered probiotics decrease Aggregatibacter actinomycetemcomitans, but not other periodontal pathogenic bacteria counts in the oral cavity: A systematic review and meta-analysis. **Frontiers in pharmacology**. https://doi.org/fphar.2021.682656
IF: 5.811

2. Ruksakiet, K., Hanák, L., Farkas, N., Hegyi, P., Sadaeng, W., Czumbel, L. M., **Sang-Ngoen, T.**, Garami, A., Mikó, A., Varga, G., & Lohinai, Z. (2020). Antimicrobial Efficacy of Chlorhexidine and Sodium Hypochlorite in Root Canal Disinfection: A Systematic Review and Meta-analysis of Randomized Controlled Trials. **Journal of endodontics**, 46(8), 1032–1041.e7. https://doi.org/10.1016/j.joen.2020.05.002
IF: 4.171

3. Sadaeng, W., Márta, K., Mátrai, P., Hegyi, P., Tóth, B., Németh, B., Czumbel, L. M., **Sang-Ngoen, T.**, Gyöngyi, Z., Varga, G., Révész, P., Szanyi, I., Karádi, K., & Gerber, G. (2020). γ-Aminobutyric Acid and Derivatives Reduce the Incidence of Acute Pain after Herpes Zoster - A Systematic Review and Meta-analysis. **Current pharmaceutical design**, 26(25), 3026–3038. https://doi.org/10.2174/1381612826666200605120242
IF: 3.116

4. Csupor, D., Viczián, R., Lantos, T., Kiss, T., Hegyi, P., Tenk, J., Czumbel, L. M., **Thanyaporn, S. N.**, Gyöngyi, Z., Varga, G., Gerber, G., Pétervári, E., & Tóth, B. (2019). The combination of hawthorn extract and camphor significantly increases blood pressure: A meta-analysis and systematic review. Phytomedicine : international journal of phytotherapy and phytopharmacology, 63, 152984. https://doi.org/10.1016/j.phymed.2019.152984
IF: 4.268

DOI:10.14753/SE.2022.2709

Acknowledgments

Firstly, my warmest thanks go to the most important persons in my life, my parents: Wipawan and Chatchawan Sangngoen, for their patience, sacrifice, and support in every step of my life. My warmest thanks also go to my brother, Tanachat Sangngoen, for the encouragement and suggestions. Unforgettable, my thanks go to my best friend, Varinthon Thubphakdee, who always shares my happiness and sadness and gives suggestions and soul support.

I express my sincere gratitude to my tutor, Professor Dr. Varga Gábor, my tutors, for the opportunity in sciences, guidance, and help throughout my Ph.D. program.

I express my special thanks to another tutor, Dr. Anna Földes for her guidance and support in my project and Ph.D. study and her help in some difficulties living in Hungary.

I acknowledge my indebtedness and a deep sense of gratitude to Dr. Martin C. Steward whose valuable guidance, advice, and help in completing my project and thesis.

I sincerely thank Dr. Beáta Kerémi for her help in laboratory works, meta-analysis project, and miscellaneous in my study.

I thank Dr. Róbert Rácz for his friendship and help in the laboratory work throughout the project.

My thanks also go to all colleagues in the Department of Oral Biology, Dr. Ákos Zsembery, Dr. Kristóf Kádár, and Dr. László Márk Czumbel, for the help and suggestions.

I thank Naresuan University for its financial support in this Ph.D. study.

I also thank all my family members, friends, and colleagues not listed here for their advice, friendship, and support.

Lastly, thanks to my supportive boyfriend, Vince Oláh, for his love, care, and patience, which energized me to pass every obstacles during my study and daily life.